

**Koninklijk Meteorologisch Instituut van België**  
**Institut Royal Météorologique de Belgique**  
**Royal Meteorological Institute of Belgium**

---



## **The INCA-BE system: ten years of operational nowcasting and its applications at the national meteorological service of Belgium**

**Maarten Reyniers<sup>1</sup>,  
André Simon<sup>2</sup>, Laurent Delobbe<sup>1</sup>,  
Alex Deckmyn<sup>1</sup>, Edouard Goudenhoofd<sup>1</sup>**  
<sup>1</sup>Royal Meteorological Institute of Belgium  
<sup>2</sup>Hungarian Meteorological Service

**2021**

Wetenschappelijke en  
technische publicatie  
N<sup>r</sup> 67

Uitgegeven door het  
**KONINKLIJK METEOROLOGISCH  
INSTITUUT VAN BELGIE**  
Ringlaan 3, B-1180 Brussel  
Verantwoordelijke uitgever: Dr. D. Gellens

Publication scientifique  
et technique  
N<sup>o</sup> 67

Edité par  
**L'INSTITUT ROYAL METEOROLOGIQUE  
DE BELGIQUE**  
Avenue Circulaire 3, B-1180 Bruxelles  
Editeur responsable: Dr. D. Gellens

**The INCA-BE system: ten years of operational nowcasting and  
its applications at the national meteorological service of Belgium**

**Maarten Reyniers, André Simon, Laurent Delobbe, Alex Deckmyn, Edouard Goudenhoofd**

*Scientific committee:*

dr. Dieter Poelman

dr. Nicolas Clerbaux

dr. ir. David Dehenauw

DOI: [10.5281/zenodo.5798952](https://doi.org/10.5281/zenodo.5798952)

Koninklijk Meteorologisch Instituut van België  
Institut Royal Météorologique de Belgique  
Königliches Meteorologisches Institut von Belgien  
Royal Meteorological Institute of Belgium

# Contents

<b>Abstract</b>	<b>5</b>
<b>1 Introduction</b>	<b>6</b>
<b>2 INCA-BE: general characteristics</b>	<b>8</b>
2.1 Domain . . . . .	8
2.2 Modular structure . . . . .	8
2.3 Input data . . . . .	9
2.3.1 NWP data . . . . .	9
2.3.2 Surface station observations . . . . .	11
2.3.3 Radar-based quantitative precipitation estimation . . . . .	13
2.3.4 Lightning data . . . . .	14
2.3.5 Satellite products . . . . .	14
2.4 Output . . . . .	15
<b>3 Extensions to the precipitation module</b>	<b>17</b>
3.1 Lightning nowcast . . . . .	17
3.1.1 Definitions and method . . . . .	17
3.1.2 Verification . . . . .	17
3.2 Hail nowcast . . . . .	21
3.3 Clear air filter . . . . .	23
3.4 Neighbourhood processing as a proxy for forecast uncertainty . . . . .	23
<b>4 Addition of a wind gust module</b>	<b>25</b>
<b>5 From raw output to forecast applications</b>	<b>27</b>
5.1 INCA-BE web portal for the RMIB forecasters . . . . .	27
5.2 Integration in the RMIB smartphone app . . . . .	27
5.3 Return period forecast (INCA-IDF application) . . . . .	27
5.4 Smartphone notifications for hazardous weather . . . . .	30
5.5 An interactive, visual monitoring of all model output at RMIB . . . . .	32
<b>6 Overall evaluation</b>	<b>34</b>
<b>7 Conclusions and outlook</b>	<b>35</b>
<b>Acknowledgments</b>	<b>36</b>
<b>List of acronyms</b>	<b>37</b>
<b>References</b>	<b>38</b>



---

## Abstract

Operational nowcasting systems are often key elements in meteorological services worldwide, e.g., in issuing severe weather warnings. Unfortunately, the documentation on these systems is not always available, which – on its turn – slows down the development and the international collaboration in this field. This technical publication is an endeavour to fill this gap between research and operations by describing the recent improvements in INCA-BE, the operational nowcasting system of the Royal Meteorological Institute of Belgium (RMIB). Several of the recently developed system extensions are discussed, including: the nowcast of lightning, the nowcast of hail, the generation of an uncertainty plume in the precipitation forecast, and the nowcast of 10m wind gusts. The INCA-BE output is exploited in numerous downstream applications, of which two are discussed in more detail: (1) a tool to detect hazardous precipitation accumulations by a real-time combination of the precipitation nowcast and return period information; (2) a unique system allowing human intervention in the generation and dissemination of smartphone notifications for severe weather. These recent developments contribute to the refinement of both the manual and automatic warnings for meteorological hazards in Belgium, not only at RMIB itself, but also in the regional hydrological and road management services.

*Important note to the reader: this technical publication describes the state of the INCA-BE system as of September 2021. While the general framework, the I/O and the main capabilities of the INCA-BE system are largely fixed, the system is actively maintained and regularly improved with new additions and extensions.*

## 1 Introduction

Meteorological services worldwide experience an ever increasing demand of forecasts with short lead-times (nowcasts) with a high temporal and spatial resolution and a high update frequency. In its classical definition, nowcasting spans the forecast range from 0 h to 6 h ahead (WMO, 2017), but many nowcasting systems have their proper maximum lead time (Reyniers, 2008). In the last decade, nowcasting products have become increasingly important for several economical sectors and public authorities (e.g., renewable energy sector, water authorities, civil protection, etc. . .). Additionally, more and more nowcasting applications find their way to the broad public through mobile devices and platforms (Zabini, 2016).

To satisfy this demand, the Royal Meteorological Institute of Belgium (RMIB hereafter) started the implementation of the INCA system back in 2010. INCA (acronym of Integrated Nowcasting through Comprehensive Analysis, see Haiden et al., 2011, for a detailed description) is a nowcasting system that has been developed at the meteorological service of Austria (ZAMG). The original system, hereafter referred to as the “INCA core system”, was adapted for a domain covering Belgium and for RMIB’s observational data flow. It was integrated in RMIB’s operational chain in spring 2012. It was first used internally by the RMIB forecasters, and later on also by some external users like the regional hydrological services. Currently, the output has found its way to numerous downstream applications and users.

An ambitious European program to promote INCA in the Central European region ran from April 2010 till September 2013: INCA-CE (Wang et al., 2017). The main goal of INCA-CE was to stimulate the use of INCA in Central Europe and to contribute to a better transnational weather information exchange between nowcasting developers and end-users, using state-of-the-art nowcasting techniques. During this program, several meteorological services in Europe have implemented INCA as nowcasting tool including Slovakia, Slovenia, Czech Republic (Kyznarov et al., 2013), Poland (Jurczyk et al., 2015) and the Italian region of Friuli Venezia Giulia. Although numerous developments from several partners were realised during the INCA-CE project, there was no common code repository foreseen for the partners, resulting in several national “forks” of the INCA core system provided by ZAMG. A probabilistic version of INCA has also been developed within the PROFORCE project (Wastl et al., 2018) and tested at ZAMG and at the Hungarian Meteorological Service (Országos Meteorológiai Szolgálat, OMSZ hereafter), in cooperation with civil protection authorities.

We would like to stress that the scope of this publication is confined to the discussion of the improvements and additions developed and implemented at RMIB on top of the INCA core system, and to the use of INCA-BE in the generation of warnings and alerts for meteorological hazards. For a comprehensive discussion of the INCA core system itself, we refer to the technical document provided by ZAMG (Haiden et al., 2010). In the current document, we limit ourselves to a brief summary of the principles and methods on which the INCA core system is built upon. Additionally, verification results of the different modules included in this core system can be found in Section 5 of Haiden et al. (2011). The outline of the publication is as follows: the general characteristics of the nowcasting system, including a concise overview of the INCA core system principles, are given in Section 2. Section 3 describes the specific additions to the precipitation module, while Section 4 discusses the completely new wind gust module that was developed at OMSZ and successfully integrated into INCA-BE. Section 5 discusses a few downstream applications based on the INCA-BE output. It starts with a short presentation of

the INCA-BE front-end that was developed for the RMIB forecasters. Then, two downstream applications developed outside the INCA-BE framework are discussed in more detail: a return period forecast obtained by combining the INCA-BE precipitation nowcast with Intensity-Duration-Frequency (IDF) information, and the generation of smartphone notifications for severe weather. A more general discussion on the strengths and weaknesses of the nowcasting system is given in Section 6. In the final Section 7, we summarise the main achievements discussed in this publication, and present the potential future development tracks.

## 2 INCA-BE: general characteristics

In Fig. 1, a general, high-level overview is given of all input/output components of the INCA-BE nowcasting system. The different components are shown as separate boxes, and are discussed in the section given in brackets on the figure. Fig. 1 is intended as a guideline throughout the entire document.

### 2.1 Domain

INCA-BE covers a domain of  $600 \times 590$  km<sup>2</sup> with 1 km resolution ( $601 \times 591$  grid points) in a “Belgian Lambert 2008” projection (EPSG:3812). The INCA-BE domain does not cover only Belgium, but also Luxembourg, the Netherlands (almost entirely), the north of France, a large part of western Germany and the southeast coast of the U.K. A significant part of the domain (19 percent) lies over sea (the North Sea and the Channel). The borders of the INCA-BE domain are shown in red in Fig. 2.

### 2.2 Modular structure

The software suite behind the nowcasting system follows a modular structure. The main programs are stand-alone routines written in Fortran and C, while the execution of these routines is controlled by shell scripts. These scripts are considered as the top-level modules of INCA-BE, and are identified with a two-letter code. For most of the modules, this two-letter code is inferred from the abbreviation classically used in the encoding of synoptic messages. INCA-BE consists of the following top-level modules:

- TQ** temperature and humidity at 2m (contraction of ‘TT’ for temperature and ‘QQ’ for humidity)
- UV** mean wind at 10m (contraction of ‘UU’ and ‘VV’, the U and V wind components)
- FF** wind gusts at 10m
- TG** ground temperature
- CH** wind chill
- RR** rain amount
- CO** convective fields
- SP** cloudiness and visibility (abbreviation of Solar Percentage)

In Table 1 an overview of the modules and their corresponding output fields is given, together with some other characteristics, like the update frequency and the forecast range.

Apart from the newly developed wind gust module (Section 4), the modular structure of INCA-BE is identical to the structure of the INCA core system. The rest of this subsection is devoted to a brief discussion of the nowcasting principles on which the INCA core system is built upon. It is a very concise summary of the comprehensive description of the system found in Haiden et al. (2010, 2011).

For temperature, humidity and wind, the three-dimensional analyses in the INCA core system start with the NWP forecast as a first guess. This first guess is corrected based on the differences between the observations and the NWP forecast at surface station locations. The NWP forecasts, interpolated to the INCA grid, are used as a background field on which ob-

ervation increments are superimposed and interpolated. The INCA forecast of these fields consists of the analysis plus the parameter change predicted by the NWP forecast. Obviously, this simple approach does not generally converge towards the NWP forecast for longer lead times. Therefore, the final INCA forecast is a weighted mean between the simple approach and the NWP forecast itself, in the form of a negative-exponential asymptotic approach.

The nowcast of ground temperature heavily relies on the output of the temperature module. First, the difference between the observed ground and 2m temperature at station locations is determined and spatially interpolated, and then this intermediate field is added to the INCA 2m temperature analysis field. The forecast of ground temperature follows the same principle of superposing the NWP trend to the analysis, but weighted with the actual NWP values, assuring convergence towards these NWP values in the long run.

For precipitation, a different nowcasting strategy is followed. In the INCA core system, the precipitation analysis is a combination of station data interpolation including elevation effects, and radar data. In INCA-BE, the principle of combining these two data sources is preserved, but the merging procedure and other radar processing are accommodated in the RADQPE product (Section 2.3.3). The INCA precipitation forecast consists of two components: (1) an observation-based extrapolation, and (2) an NWP model component. Motion vectors are inferred from consecutive precipitation analyses, are filtered by using the NWP wind field, and are applied to the latest RADQPE radar field to obtain the precipitation forecast. Additionally, the NWP precipitation prediction is injected into the INCA precipitation forecast from a lead time of +2 hours onward.

For cloudiness, the nowcasting strategy is similar as for precipitation, in the sense that no NWP model output is used in the analysis step, but information obtained by remote sensing. The cloudiness analysis in INCA is an analysis of insolation fraction based on station observations, using MSG cloud type data for spatial interpolation. The cloudiness forecast is similarly based on motion vectors derived from consecutive analyses, but in INCA-BE the motion vector calculation from the INCA core system is replaced by the extrapolation produced by the SAFNWC software suite (see Section 2.3.5, for more details).

Finally, the modules for wind chill and convection are essentially post-processing modules that are using the output of the modules discussed above.

## **2.3 Input data**

High quality input data are essential for any nowcasting system, as they provide the basis on which the nowcast is built upon. A comprehensive description of all input sources used in INCA-BE is given in this section. Table 1 specifies which input sources are used for the different modules.

### **2.3.1 NWP data**

It is clear from Table 1 that output from numerical weather prediction (NWP) models is a crucial building block for almost all modules in INCA-BE. The NWP output used in INCA-BE is the one of ALADIN/ALARO (Termonia et al., 2018), a limited area model with hydrostatic dynamics.

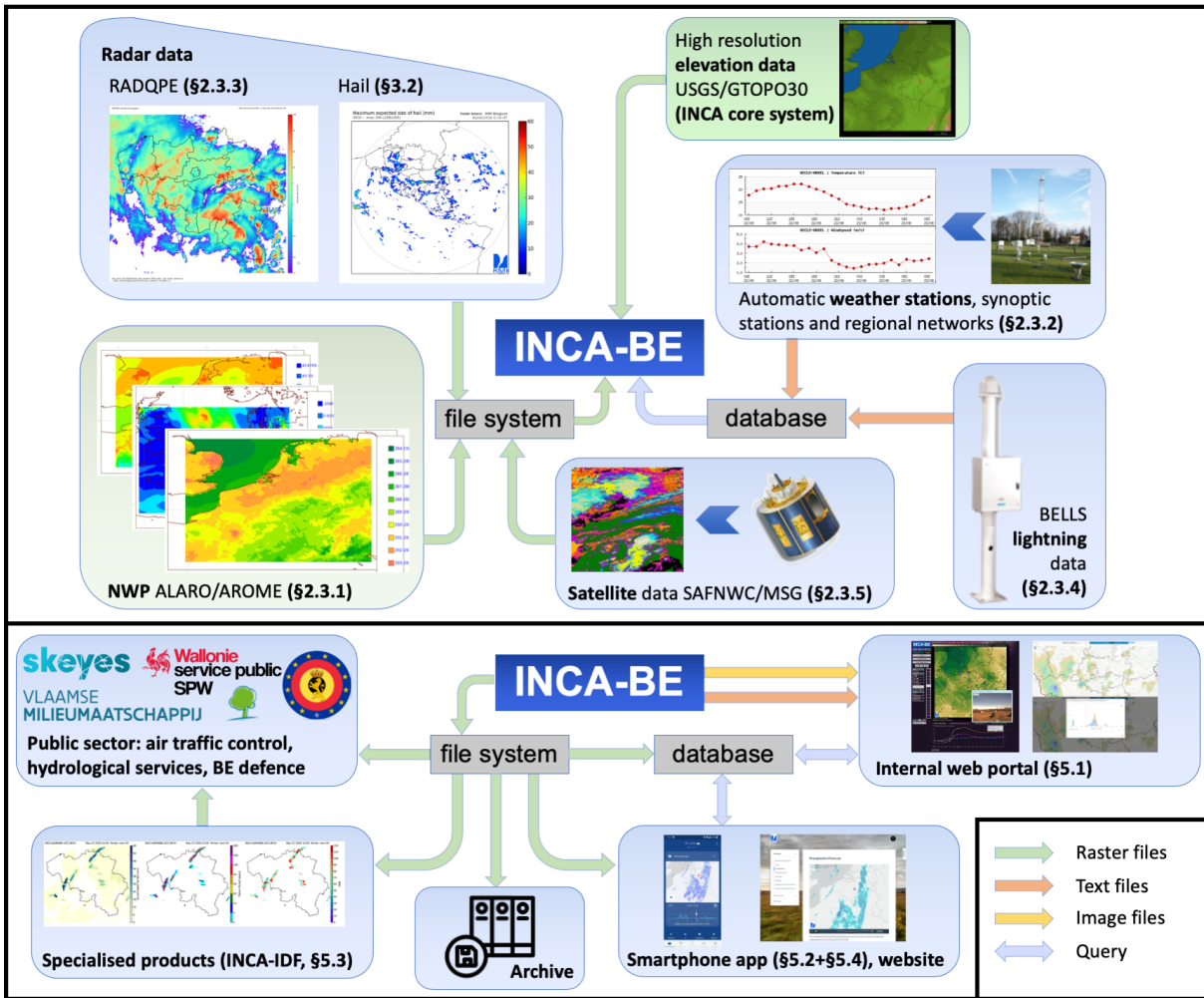


**Figure 1:** High-level overview of all input (top panel) and output (bottom panel) components of the INCA-BE nowcasting system. For every component, the relevant section number is added in brackets, if available. The colour of the arrow represents the nature of the data flow, and is specified in the legend in the bottom right corner.

Four ALARO forecast runs per day are performed operationally at RMIB (00Z, 06Z, 12Z, 18Z), and are integrated to +60 h. The model has a 1 h output frequency, and a spatial resolution of 4 km, with 87 vertical levels. Post-processed fields are available roughly four hours after analysis time. Initial conditions and boundary conditions are from the global model ARPEGE (Météo-France). The 4 km ALARO model is currently running as dynamical downscaling (hence without local data assimilation). Local data assimilation is planned for 2022.

Both two-dimensional and three-dimensional ALARO output fields are ingested into INCA-BE. The 3D-fields include geopotential, temperature, relative humidity and the three wind components  $u$ ,  $v$  and  $w$ . These fields are provided on 15 pressure surfaces with a vertical resolution of 25 hPa up to 900 hPa, 50 hPa up to 700 hPa, and a resolution of 100 hPa above. The 2D-fields from ALARO that are fed into the INCA-BE system are: 2m temperature and relative humidity, the  $u$  and  $v$  10m wind components, precipitation, total cloudiness, global radiation, and surface temperature.

In April 2020, an independent, parallel INCA-BE suite was set up that ingests the recently implemented 1.3 km AROME model output (Seity et al., 2011) as base NWP. The RMIB implementation of AROME adds local surface data assimilation. This parallel INCA-BE suite is, however, not considered as operational, as it is still in test phase. There are currently no downstream products depending on this parallel version, yet its output is already made available to the forecasters at RMIB for evaluation purposes. This parallel INCA-BE suite will not be further discussed in the current publication.

### 2.3.2 Surface station observations

Temperature, dew point, humidity and wind data are extracted from RMIB's surface station observations database every hour. This database contains data from several station networks. For the Belgian territory, these include not only the 17 automatic weather stations (AWS) of the RMIB network, but also the stations operated by Skeyes (the Belgian air safety authority) and the stations operated by the meteorological wing of the Belgian Air Force. The total number of Belgian stations for which hourly data is available in near-real time is around 30. Due to a bilateral agreement on real-time data exchange with Dutch weather service KNMI, INCA-BE ingests also the 42 stations within the INCA-BE domain from the Dutch AWS network.

For other neighbouring countries, the synoptical stations are used, including stations at ships, buoys and platforms. The delay in the reception of these data is somewhat larger, but generally we find that roughly 110 foreign stations inside the INCA-BE domain are available within 25 min. Due to the time delay between the domestic and the foreign stations, we decided to perform two independent INCA-BE runs of the hourly fields (Table 1) each hour. The first run is scheduled at  $T+09\text{min}$ , the second at  $T+42\text{min}$ . The first run provides a quick view on the passed hour and a preliminary forecast, mainly intended for time-critical nowcasting purposes, while the second run is based on a larger number of stations and hence provides more accurate analyses and forecasts.

Contrary to the original INCA implementation at ZAMG, at RMIB the INCA-BE ground module (INCA\_TG, see Table 1) is mainly used to produce an auxiliary field for road weather applications. This setup was tested before in the INCA-CE project (Wang et al., 2017), in which the INCA\_TG module was coupled with the road weather model METRo (Crevier and Delage,

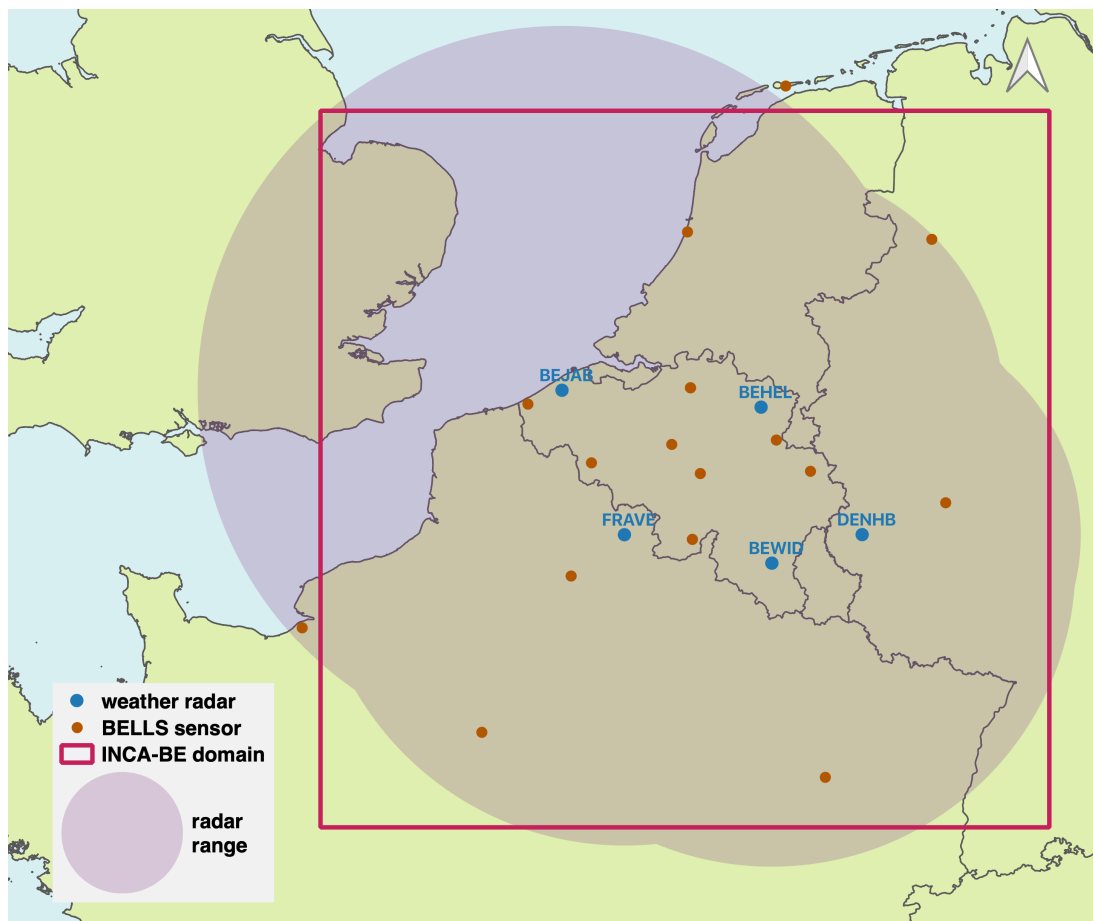


**Figure 2:** The INCA-BE domain (red rectangle) together with the locations of the weather radars (blue dots) that are included in the RADQPE composite, and the lightning sensors of the BELLs network (orange dots). These two types of instruments provide crucial input data for INCA-BE. The shaded area indicates the range of the composite radar image.

2001). At RMIB, the INCA\_TG output field is used as a base layer in RMIB's dedicated Road Weather Model (adapted from Karsisto et al., 2017) outside INCA-BE. For this purpose, an additional stream of road weather station (RWS) data was established between RMIB and the road management services in Belgium and the Netherlands (the latter one through KNMI). The number of stations included in this particular stream is considerable: 73 RWS operated by the Agentschap Wegen en Verkeer (Flanders), 49 RWS from the Service Public de Wallonie (SPW) and 319 RWS from Rijkswaterstaat (the Netherlands). Note that the INCA\_TG output is also used for the diagnosis of freezing rain in the precipitation type module (INCA\_PT, Table 1).

Since the precipitation module (INCA\_RR) runs in a 10 min cycle, the temporal resolution of the station data for precipitation should be at most 10 min as well. Similar as for INCA\_TG, a data transfer was established between the regional hydrological gauge networks in Belgium and RMIB. As a result, besides AWS data from RMIB and KNMI, data from 95 and 58 additional gauges provided by the hydrological services of the Walloon and the Flemish region, respectively, are ingested into the INCA-BE precipitation module.

### 2.3.3 Radar-based quantitative precipitation estimation

A real-time quantitative precipitation estimation map, the RADQPE product, is ingested every five minutes into the precipitation module of INCA-BE (INCA\_RR, Table 1). It is based on the measurements of five C-band weather radars (Fig. 2): the two RMIB radars in Wideumont (BEWID) and Jabbeke (BEJAB), the relatively new radar (2016) of the Flanders Environment Agency VMM in Helchteren (BEHEL), the Météo-France radar in Avesnois (FRAVE), and the DWD radar in Neuheilenbach (DENHB). It also includes the measurements from three regional gauge networks mentioned at the end of Section 2.3.2.

The RADQPE precipitation estimation is obtained after a careful processing of the raw volumetric radar reflectivity measurements, and includes the filtering of non-meteorological signals, ground rainfall estimation from radar reflectivity aloft, a merging with rain gauges and a compositing scheme. The first three components are based on the methods described in Goudenhoofd and Delobbe (2016). For the compositing, single radar rain rates are combined into a composite by taking the maximum value of the three closest radars in the convective season (May–August). In the other months, a weighted value from all radars is calculated for the overlapping areas, in which the inverse distance to the radar is taken as weight. This advanced compositing strategy reflects the general notion that radar data quality decreases with distance from the radar, except in cases of severe convection. It is able to mitigate overestimation in cases of overhanging precipitation, but at the same time it allows to fill in the attenuation on single radar images caused by strong reflectivity cores in cases of severe convection.

The composite generation in RADQPE is quite robust in the sense that the radars contained in this composite have large overlapping areas in the INCA-BE domain. Two composites with a five minute time difference are added together to synchronise with the 10 min time step of the INCA-BE precipitation module. In the near future, it is planned to use the 10 min accumulation provided by RADQPE, which includes an advection correction to take the displacement of the precipitation into account when accumulating precipitation.

The filtering of non-meteorological signals as it is done in the RADQPE product, is particularly a challenging task. The filtering must be able to remove all non-precipitation signals

to avoid false detections and warnings, and at the same time, it must be able to keep very light precipitation. In the case of snow, for example, even the detection of very light amounts is required for issuing warnings for road maintenance services. Moreover, the expansion of wireless technologies causes severe interference for weather radars and a growing number of disturbances has been observed during the last two decades. Removal of such interferences in radar observations inevitably affects the quality of rainfall detection and warnings (Saltikoff et al., 2016).

### 2.3.4 Lightning data

Starting in 1992, RMIB has a long tradition in the detection of electrical atmospheric activity by operating its own Lightning Location System (LLS). The initial network consisted of five SAFIR sensors (Surveillance et Alerte Foudre par Interférométrie Radioélectrique) exploiting the interferometry direction finding principle for the detection of both intra- and intercloud (IC), as well as cloud-to-ground (CG) discharges. Over the last ten years, the network has been completely renewed and extended by gradually replacing the SAFIR sensors with LS7002 sensors employing the time-of-arrival principle for the location of the electric discharges. In addition, sensors located in neighbouring countries were added to the state-of-the-art central Total Lightning Processor (TLP) in Brussels. In the summer of 2020, the SAFIR sensors were switched off, and the migration to this new BELLS network (BELgian Lightning Location System, Poelman et al., 2013) was completed. Due to continuous adaptation and improvement of the system with ongoing hardware and software upgrades, the median location accuracy is in the range of 100 m. The detection efficiency for negative CG strokes and flashes reaches 84% and 98%, respectively, based on video and E-field records. For more detailed information, see Schulz et al. (2016) and Poelman et al. (2016).

### 2.3.5 Satellite products

The INCA-BE cloudiness and visibility *analyses* (module INCA.SP, see Table 1) are essentially a combination of sunshine duration data from the RMIB and KNMI AWS networks and the Cloud Type (CT) product. The latter is one of the outputs of the Nowcasting Satellite Application Facility (NWC SAF) software of which an instance is running locally at RMIB. The NWC SAF is a processing chain for the Meteosat Second Generation (MSG) satellite data, with the aim of generating end-products to be used in operational meteorology and research activities. Until early 2021, the CT-product used as input in INCA-BE was generated by the NWC SAF v2013 software suite (CT-product version CT-PGE02\_v2.2, Derrien, 2014). At the end of 2020, the RMIB remote sensing team upgraded the NWC SAF software to its latest version (v2018.1), and INCA-BE was subsequently updated to use the CT-product from this new NWC SAF production chain in April 2021 (CT-product version GEO-CT-v4.0).

Along with the upgrade to NWC SAF v2018.1, the *forecast* of the cloudiness and visibility fields with a lead time of two hours was introduced as well. For its cloudiness forecast, INCA-BE takes the extrapolated CT-product generated by the Extrapolated Imagery Processor (EXIM) included in the NWC SAF suite (for details, see García-Pereda et al., 2019), and transforms it into a cloudiness field, in the same fashion as in the cloudiness analysis but without station data input. The visibility field is then consecutively calculated based on this cloudiness

forecast, and on the forecast of the other fields on which it depends (temperature, relative humidity). Note that currently the station data used in the analysis do not have any impact on the generated cloudiness forecast, and hence discontinuities between analysis and forecast are not excluded. It is however planned to introduce an additional mechanism to prevent such potential discontinuities.

The standard MSG CT-product cannot be used since its time sampling of 15 min is incompatible with the time sampling of the station data (10 min). Hence, the CT derived from the MSG Rapid Scanning Service (RSS) with a temporal resolution of 5 min is taken as input for the INCA\_SP module. During temporary RSS outages, the standard MSG products are nevertheless used, and consequently the INCA\_SP module is run every 15 min instead of every 10 min. The INCA-BE cloudiness field is additionally used in the construction of the clear air filter in the precipitation analysis (discussed in Section 3.3).

## 2.4 Output

The output fields of the different modules are listed in the rightmost column of Table 1. Raw output files are converted to the standard GRIB-1 format (WMO, 1994) for image generation, further processing in downstream applications, and dissemination to external clients. Special attention was paid to the choice of the colour maps in the image generation. In particular, the use of rainbow-like colour maps was avoided (see, e.g., Fig. 8). Rainbow or jet colour maps suffer from several deficiencies like biases and false gradients, hence they are not well suited to represent numerical data (e.g., Stauffer et al., 2015; Stoelzle and Stein, 2021). In INCA-BE the *cmocean* set of colour maps (Thyng et al., 2016) was adopted, as alternative for the rainbow colour maps. These perceptually uniform colour maps were originally developed for use in oceanography, but are now increasingly used in other geophysical domains as well.

**Table 1 :** Overview of the INCA-BE modules and fields.

Module	Time res.	Update	Forecast range	Input data	Output fields
NWP2INCA	1 h	6h	36 h	ALARO GRIB files	NWP on INCA-BE grid (auxiliary module)
INCA_TQ	1 h	2× per h	12 h	stations, NWP	2m Temperature, 2m Dew point, 2m Relative Humidity, Snowfall level, Freezing level, 3D Temperature, 3D Humidity, 3D Wind
INCA_UV	1 h	2× per h	12 h	stations, NWP	10m Wind
INCA_FF	1 h	2× per h	12 h	INCA_TQ, INCA_UV, NWP	10m Gusts
INCA_TG	1 h	2× per h	12 h	stations, INCA_TQ, NWP	Ground temperature
INCA_CH	1 h	2× per h	12 h	INCA_TQ, INCA_UV	Wind chill
INCA_RR	10 min	10 min	4h	stations, INCA_TQ, INCA_SP, NWP, radar, hail detection, lightning	Precipitation, Precipitation type, Lightning
INCA_CO	1 h	2× per h	–	stations, NWP	collection of convective analysis fields: CAPE, CIN, LCL, Level of free convection, Lifted Index, Showalter Index, Deep Convection Index, Trigger temperature, Trigger temperature deficit, Equivalent Potential temperature, Moisture convergence, Flow divergence, Precipitable water
INCA_SP	10 min*	10 min*	2 h	stations, INCA_TQ, NWC SAF	Cloudiness, Visibility

\*15 min in case of MSG RSS outage.

### 3 Extensions to the precipitation module

#### 3.1 Lightning nowcast

##### 3.1.1 Definitions and method

In order to introduce the lightning nowcast in INCA-BE, the auxiliary fields  $LA$ ,  $LS$  and  $LF$  are defined; their definitions are given in Table 2. As shown in Eq. (1), the lightning nowcast  $LF$  is a conservative advection of the  $LS$ -field, the latter one being a smoothed version of the observed lightning field  $LA$ . Note that, although these fields are binary (0/1), an area with a value of 1 in the forecast field  $LF$  should not be interpreted in a deterministic way, but as an indication of an electrically active area or a *risk zone* where lightning can possibly occur. Slightly different definitions of the lightning forecast were tested by adopting a lagged approach of past lightnings (see again Table 2 for the precise definition of the different fields and operators):

$$\begin{aligned} \underline{\text{LAG0}} \quad LF(t_0+\Delta t) &= \text{adv}(\Delta t, LS(t_0)) \\ \underline{\text{LAG1}} \quad LF(t_0+\Delta t) &= \text{adv}(\Delta t, LS(t_0) + \text{adv}(10, LS(t_0-10))) \\ \underline{\text{LAG2}} \quad LF(t_0+\Delta t) &= \text{adv}(\Delta t, LS(t_0) + \text{adv}(10, LS(t_0-10)) + \text{adv}(20, LS(t_0-20))) \end{aligned} \quad (1)$$

In words: in LAG0, LAG1 and LAG2, the lightning forecast is based on lightnings in the past 10, 20 or 30 minutes respectively.

##### 3.1.2 Verification

We used the classical categorical verification method of hits and misses as defined in Table 3. Since  $LF$  is intended to be a prediction of  $LS$ , its verification is done against  $LS$ , and not against  $LA$ . Scores for the Probability Of Detection (POD), the False Alarm Ratio (FAR) and the Critical Success Index (CSI) were calculated. In the formalism of Table 3, these are given by  $\text{POD} = a/(a + c)$ ,  $\text{FAR} = b/(a + b)$  and  $\text{CSI} = a/(a + b + c)$ .

The verification was performed on two storm episodes in 2015 with intense lightning activity: 5 June 2015 and 13 August 2015 (hereafter labeled as the 2015-06-05 case and the 2015-08-13 case, respectively). Fig. 3 contains a snapshot of the INCA-BE precipitation and lightning forecast of the 2015-06-05 case, at 17:00 UTC; this is when the storm reached maturity. On the left hand side of Fig. 3, three consecutive analysis images are given, while on the right hand side the forecast for the next 10 minutes is given for each of the three different LAG-levels (see Eq. 1). From the definition of the lagged forecast method, it is easily understood that the area covered by the lightning nowcast field ( $LF$ ) is larger for forecasts with higher LAG-levels.

In Fig. 4 the verification results are presented. POD, FAR and CSI scores are shown as a function of lead time for the two cases above, and for the different LAG-levels. The maximum lead time on these figures is set to 60 min, which is already on the long side for these convective and very dynamic situations (e.g., Foresti et al., 2016). Fig. 5 repeats the results for the 2015-06-05 case, but now separated according to the development stage of the overall lightning activity within the INCA-BE domain (intensification – mature – weakening). For this particular case, we defined the intensification phase as the time interval for which lightning activity raised

### 3. EXTENSIONS TO THE PRECIPITATION MODULE

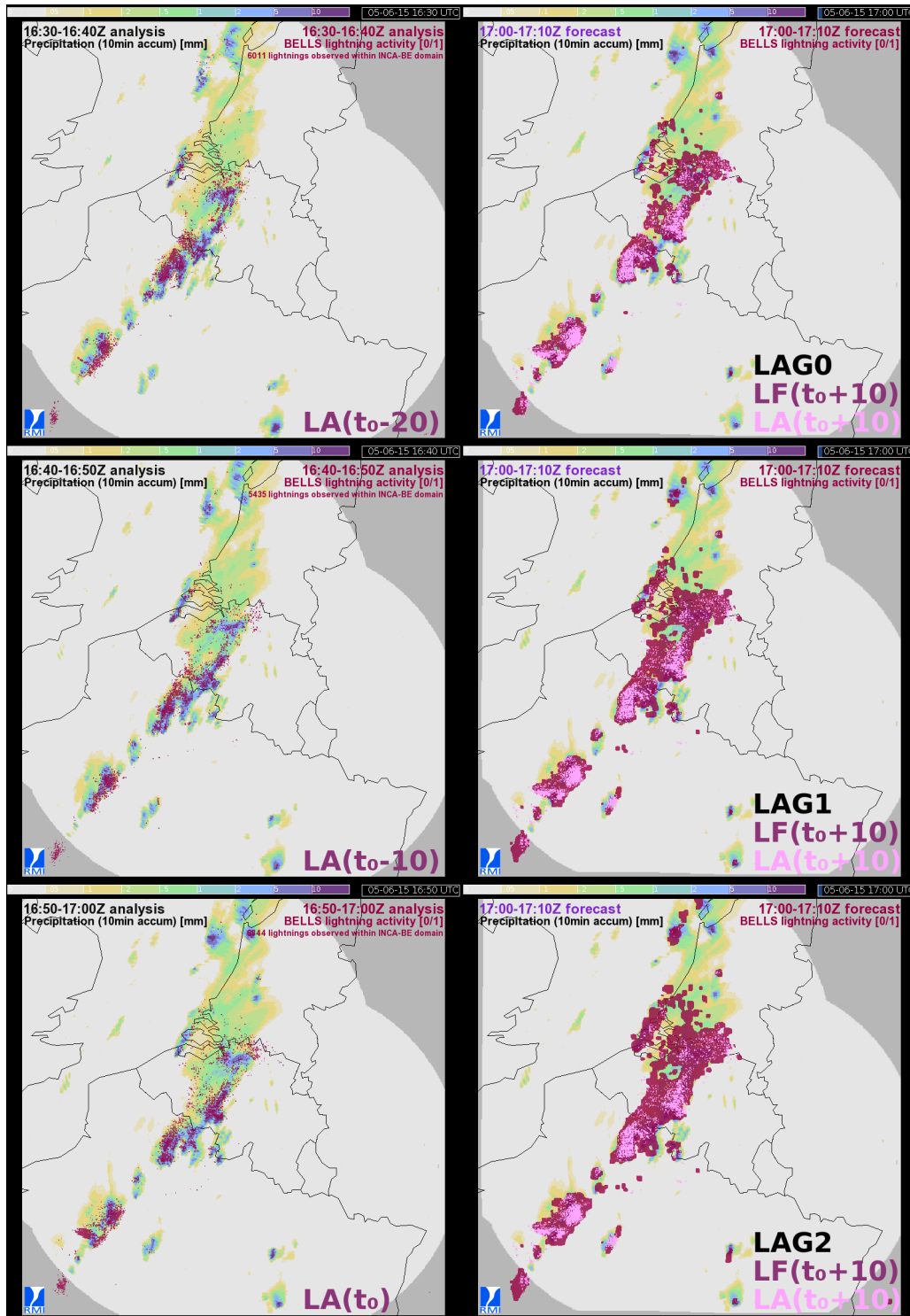


**Figure 3:** Snapshot of the INCA-BE precipitation and lightning forecast of the 2015-06-05 case at 17:00 UTC. On the left hand side, three consecutive analysis images are given. On the right hand side, the lightning forecast is shown for the next 10 minutes, generated with the three different LAG-levels (Eq. 1). For the precise definition of LA and LF, see Table 2. On the three panels on the left, the observed lightning detections (LA) are overplotted in purple. On the panels on the right, purple is used for the lightning forecast LF, while the observed (verification) lightning detections (LA) are shown in pink. The explanation of the colours is also reflected in the colour of the labels in the lower right corner. The colour scale shown on top of all panels is the scale for the precipitation amount.

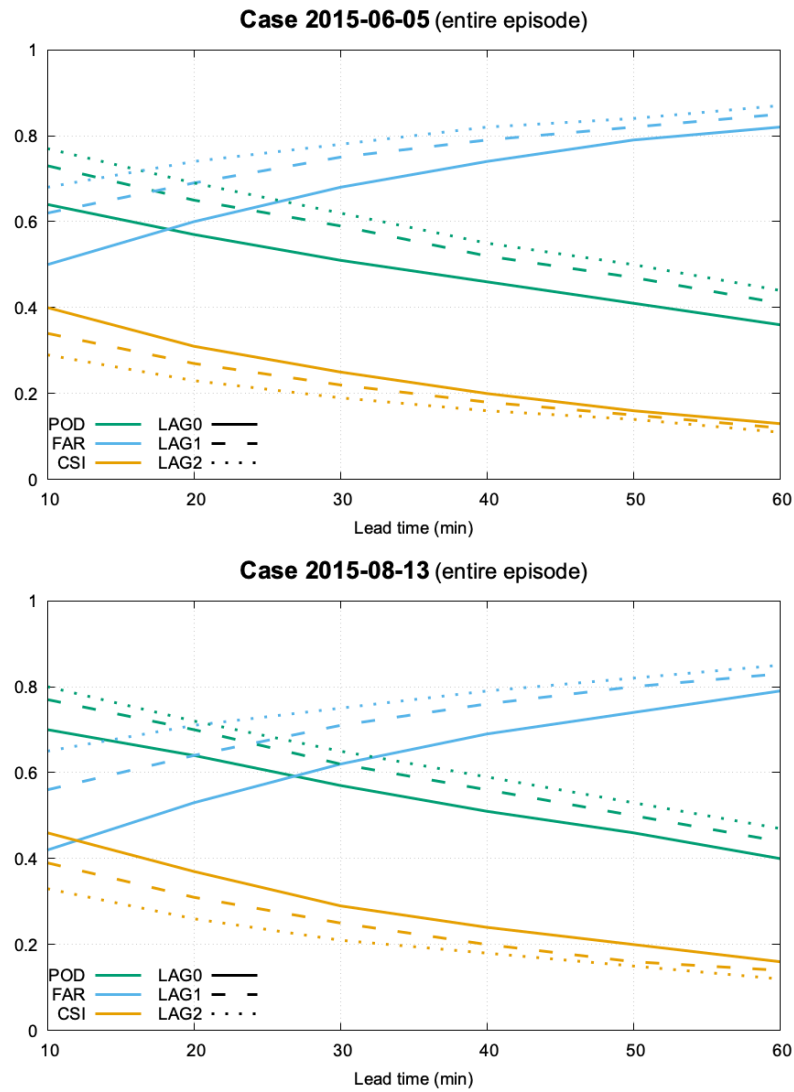


**Figure 4:** Verification of the lightning forecast for the 2015-06-05 case (top panel), and the 2015-08-13 case (bottom panel) for the entire episodes. Full, dashed, and dotted lines are used for the LAG0, LAG1 and LAG2 levels, respectively; POD, FAR, CSI are shown in green, blue, and beige, respectively.

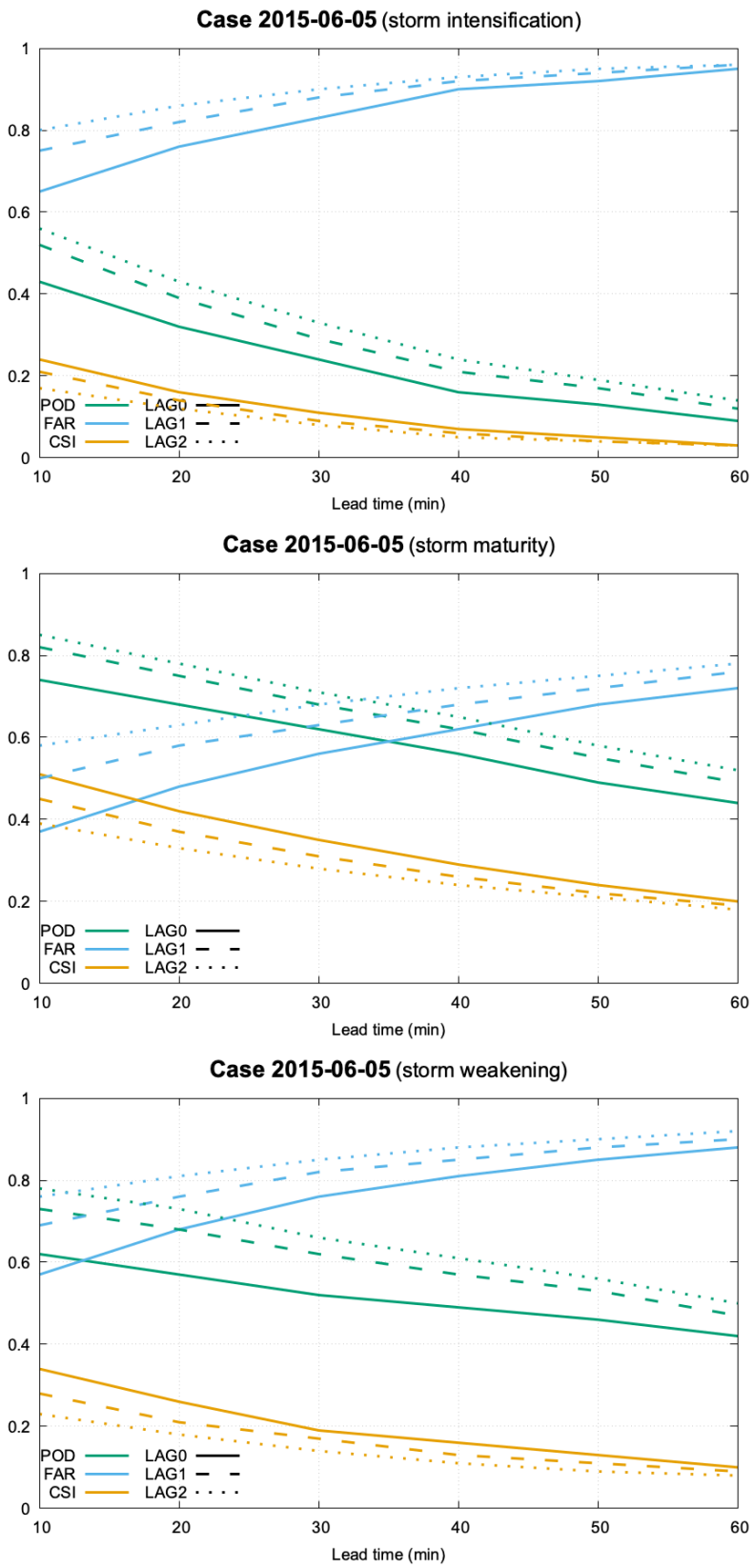


**Figure 5:** Same as the top panel of Fig. 4 (2015-06-05 case), but the respective panels now show the verification statistics for the three different phases in the storm development (intensification – mature – weakening).

**Table 2:** Definition of the fields used in the lightning nowcast.

Field	Definition
$LA(t_0)$	Binary field for the observed lightning activity at time $t_0$ , defined as 1 for a given INCA-BE grid box if at least one lightning (IC or CG, see Section 2.3.4) is observed in that box between $(t_0 - 10\text{min})$ and $t_0$ , 0 elsewhere
$LS(t_0)$	Smoothed version of $LA(t_0)$ obtained by applying a Gaussian smoothing with a kernel width of two pixels (2 km); additionally isolated lightnings are eliminated, and adjacent lightnings are connected
$LF(t_0+\Delta t)$	Forecast of field $LS$ issued at time $t_0$ with valid time $t_0+\Delta t$
$adv(\Delta t, Y)$	Forward advection of field $Y$ with $\Delta t$ minutes. Advection vectors are taken from the precipitation nowcast.

**Table 3:** Classical contingency table for categorical verification.

LF \ LS	1	0
1	$a$ (hits)	$b$ (false alarms)
0	$c$ (misses)	$d$ (correct neg.)

from 50 to 3000 detections (the sum of IC pulses and CG strokes, see Section 2.3.4) per 10 minutes within the entire INCA-BE domain; the mature phase was defined as the interval with more than 3000 detections per 10 minutes; and the weakening phase as the phase for which the activity dropped again below 3000 detections per 10 minutes.

Since there is no prediction of lightning initiation, the verification scores during thunderstorm development are rather low. Additionally, small cells are typically short-lived, which will have an impact on the scores as well. A forecast with more “memory” (higher LAG-level) results in a higher detection probability (POD), but unfortunately the number of false alarms is increasing even more. The net effect are CSI scores that are slightly decreasing for more conservative forecasts, i.e.,  $CSI_{LAG0} > CSI_{LAG1} > CSI_{LAG2}$ . Nevertheless, for critical applications (e.g., airport operations), a forecast with a higher lag-level can be the preferred forecast, due to its higher probability of detection. Since the output of INCA-BE is also provided to the Belgian aviation safety authority Skeyes, a lightning forecast of LAG-level 2 is chosen in the operational version of INCA-BE.

### 3.2 Hail nowcast

The precipitation type classification included in the INCA core system contains only three classes (rain, snow and a mixed state), with an additional diagnosis for freezing rain (Haiden et al., 2010). In order to extend the usability of the INCA precipitation type field towards the summer months, the INCA\_RR module (Table 1) was combined with the output of the radar-based hail detection algorithms that are operational at RMIB. More specifically, two hail detection algorithms are currently implemented at RMIB (Lukach et al., 2017):

- Holleman’s version of Waldvogel’s algorithm for the Probability Of Hail (POH, Holleman 2001);

- Witt's algorithm estimating the Probability Of Severe Hail (POSH), i.e., hail with a diameter of at least 20 mm (Witt et al., 1998).

Based on the output of these algorithms, we added a conservative hail forecast to INCA-BE. This includes the following steps. First, the POH and POSH fields are converted to deterministic, binary (yes/no) fields by applying a threshold to the probabilities. The threshold in this procedure was determined after a feed-back loop with the RMIB forecasters and is now fixed at 65%. Then, these “binary” POH and POSH fields are advected using the INCA-BE vector field derived from the radar images; see Haiden et al. (2010) for a description of the advection in INCA. Finally, these advected fields are added to the appropriate time step of the original INCA precipitation type forecast.

The precipitation type field in INCA-BE is hence a blending of a rain/snow *prediction* (from the INCA core system) and a hail *advection* (added in INCA-BE). Contrary to the snow prediction, hail is not generated in the nowcast: it is only an advection of observed hail at  $t_0$ . This heuristic method is based on the observation that hail cores are often associated with mesoscale convective systems (MCSs) or with supercells, and these systems are generally long-lived.

The verification of a hail forecast is particularly challenging due to the scarcity of ground truth data. The traditional verifying data used for hail detection and forecasts are very heterogeneous and originate from, e.g., damage reports to insurance companies, e.g., Debontridder (2008), or from articles in the media. While these sources of information are certainly useful, they suffer from several shortcomings. Articles in the media for example tend to be biased to the more extreme cases, and – in the case of social media – the information provided is very subjective or contains errors, e.g., Fohringer et al. (2015), Brouwer et al. (2017), Spruce et al. (2021), for studies on flood reports through social media. More fundamentally, it suffers from the fact that it does not contain non-events, i.e., it cannot reject forecasted hail events that did not occur.

In an attempt to overcome these issues, more and more meteorological services are exploring citizen science and crowdsourcing approaches that are more homogeneous by design. In this context, RMIB has added a reporting tool in its smartphone app, inspired by comparable initiatives like “mPing” (Elmore et al., 2014), the “EWOB” app of the European Severe Storms Laboratory (ESSL), the app of Finnish Meteorological Institute (“FMI Weather”), the one of Météo-France, and the one of MeteoSwiss (only hail report). With this reporting tool, users are able to send a meteorological observation to RMIB with some simple taps on his/her mobile device, through a clean and attractive interface. While this information collection strategy also suffers from possible pollution by forged observations and from a population density bias, it is a considerable step forward in the homogenisation and standardisation of the verifying data set.

The reporting feature was added in the RMIB smartphone app in August 2019, and currently (September 2021) around 1,9 million reports were collected (on a total population of 11,5 million inhabitants in Belgium). Hail is only one of the fourteen possible observation types that can be reported, and currently our database holds around 12300 hail reports. Although this is already a fair amount of reports, a data collection over several hail seasons is recommended to perform a thorough verification study of the hail detection and forecast. In Switzerland, Barras et al. (2019) used more than 50,000 crowdsourced hail reports to evaluate the quality of radar-based hail detection. Contrary to the setup of MeteoSwiss, also rain reports are collected in the RMIB

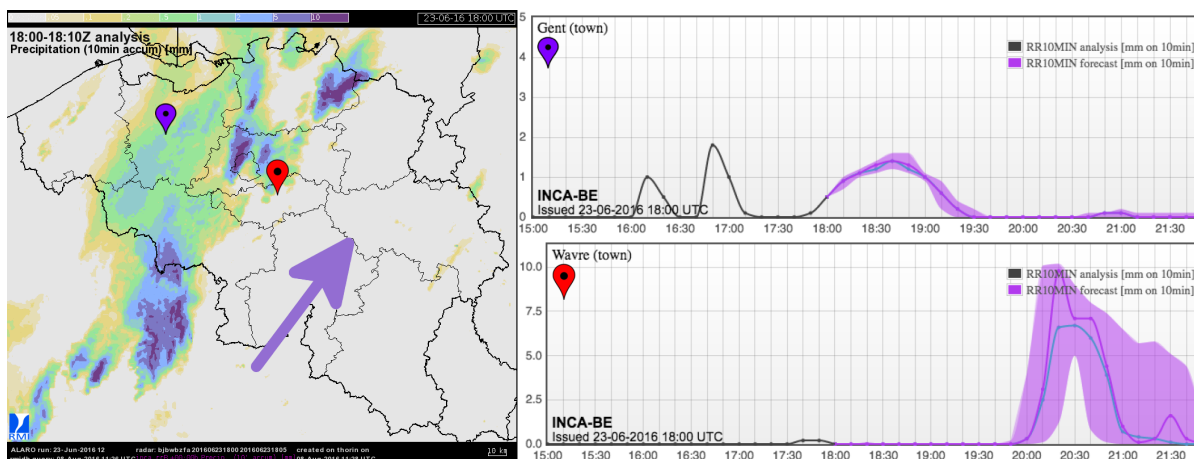


**Figure 6:** Precipitation meteograms for two locations, Gent (purple marker) and Wavre (red marker), for a convective situation on 23 June 2016. Gent (upper right panel) is located in a more stratiform zone (low uncertainties, narrow plume), while Wavre (lower right panel) is expected to be hit by some convective cells (high uncertainties, broad plume). The main storm movement is indicated by the big purple arrow on the map. The meteograms show both the deterministic forecast (purple line) as well as the median of the surrounding locations (blue line).

app, which allows to produce an estimate of the false detections as well.

Currently we are in the process of refining the quality control procedures of our data flow, while carrying out some preliminary tests on the data set collected during the hail season of 2020. A preliminary analysis of the 1956 hail reports received in the period May-September 2020 resulted in a first estimate of the hail detection efficiency of the radar with this new data set: almost 90% of the hail cases are detected by the POH algorithm. These first results are in line with earlier findings concerning the detection efficiency of the radar for hail by Delobbe et al. (2005), which made use of 83 reports of weather amateurs and articles published in newspapers.

### 3.3 Clear air filter

The INCA core system contains a satellite filter to clean the input of the precipitation field from possible non-meteorological echoes remaining after the RADQPE processing. It takes as input the cloudiness field of the INCA\_SP module (Table 1), and removes any nonzero precipitation values in clear sky areas. A precipitation value is set to zero in a given location if the maximum cloudiness does not exceed 20% in an area of 10 km around that location. This basic satellite filter included in the INCA core system was improved by applying an advection on the latest available cloudiness field, to match the timing of the precipitation module. This advection is necessary since the radar imagery, on which the precipitation module is based, generally arrives faster than the satellite images needed in the cloudiness module.

### 3.4 Neighbourhood processing as a proxy for forecast uncertainty

The spatial variation of the rainfall field is taken as a proxy for the predictability of the precipitation forecast. Uncertainty plumes are added to the precipitation meteograms by assessing

the variability of the forecast values in the direct vicinity of the location. This “vicinity” is defined as the collection of pixels within a certain radius, which is increasing with increasing lead time: +0.5 km per 10 min increase in lead time, starting from radius=0 in the analysis step. Pixel values within this radius are ordered and the plume is constructed by the [5;95] percentiles. Two examples of such meteograms are shown in Fig. 6.

This heuristic method of estimating the uncertainty of the precipitation forecast is based on the observation that small scale features in a rainfall field are much less predictable than large scale, more stratiform structures (see, e.g., Fig. 8 in Seed, 2003). However, post-processing a Lagrangian prediction like it is done here, will not properly account for growth and decay of the precipitation field, and therefore offers only a rough indication of the uncertainty. The proper way of quantifying the uncertainty in a precipitation nowcast is by generating an ensemble of possible future rainfall scenarios. Such a probabilistic nowcasting system, in which the deterministic radar extrapolation is perturbed with stochastic noise to produce an ensemble of varying but equally probable precipitation nowcasts, is currently pre-operational at RMIB (STEPS-BE, Foresti et al., 2016).

Probabilistic precipitation nowcasting will be further developed under the umbrella of RMIB’s seamless prediction program “IMA” (De Cruz et al., 2020). The framework in which these developments are pursued is PySTEPS (Pulkkinen et al., 2019a,b), a community driven open-source Python library for probabilistic precipitation nowcasting. PySTEPS is built on the same principles as the original STEPS system, but in addition it supports various input/output file formats and implements several optical flow methods. Also important additions were introduced in the stochastic noise generation, visualisation and forecast verification. It is foreseen that PySTEPS becomes the main precipitation nowcasting system at RMIB in the future. Hence, the current plume presented here will be replaced with the plume produced by the ensemble of forecasts generated by a local instance of PySTEPS, in which also the blending with the NWP model will be handled.

## 4 Addition of a wind gust module

The wind gust parameterisation has been developed in the frame of the INCA-CE project (Wang et al., 2017). In this scheme the forecast gusts are primarily products of large-scale circulation wind and turbulence parameterisation. Similar approaches based on first order turbulence closure have already been used in NWP models and nowcasting systems (Sheridan, 2011). These can be directly applied with standard nowcasting parameters (wind and temperature profiles) on input and their processing is fast. The parameterisation does not simulate wind gusts related to deep convection (which was tested within the INCA-CE project separately). The formula for the wind gust  $G_u$  yields:

$$G_u = (1 + c'_n C_{DI}) |\vec{v}| \quad (2)$$

where  $|\vec{v}|$  is the 10 m wind speed,  $c'_n$  is a constant (equal to 5.2) and  $C_{DI}$  is the square root of the drag coefficient for momentum. The latter parameter depends on the bulk Richardson number  $Ri$ , which represents the stability of the lowest 20 m height above the surface:

$$C_{DI} = L_{fr} C_n \sqrt{F(Ri)} \quad (3)$$

In this equation,  $C_n$  is the square root of the surface drag coefficient for neutral stratification (Louis et al., 1982),  $L_{fr}$  can be modified separately for stable/unstable conditions, and is currently set to 1.4. The Richardson number function  $F(Ri)$  is different for stable and unstable near-surface layer and it was used in former ECMWF and ALADIN parameterisations of turbulent fluxes (see the formulas 1b and 3a in Louis et al. 1982).

The original parameterisation defined by Eqs. 2 and 3 had the drawback of a very fast increasing gust factor (ratio of the gust and 10 m wind speed) with decreasing  $Ri$  in unstable conditions (Fig. 7). This can cause unrealistically high gusts in case of strong winds (Simon et al., 2012). For this reason, the Eqn. 3 has been modified:

$$C_{DI} = L_{fr} F_{\text{mod}} C_n \sqrt{F(Ri)} \quad (4)$$

In stable conditions,  $F_{\text{mod}} = 1$ . In unstable conditions ( $Ri < 0$ ) the function yields:

$$F_{\text{mod}} = \frac{1}{1 + k_1 Z_{0f} \sqrt{-Ri}}, \text{ where} \quad (5)$$

$$Z_{0f} = 1 + k_2 \ln \left( 1 + \frac{Z_0}{Z_{0\text{max}}} \right) \quad (6)$$

The modification of the gust factor depends on the roughness length  $Z_0$  and it can be controlled by parameters  $k_1$  and  $k_2$  (set to 0.13 and 1.5, respectively). The roughness length is limited to 1 m ( $Z_{0\text{max}}$ ). The gust factor in the modified scheme involving Eqs. 4 and 5 can vary between 1 and 2.5, which is observed in most of the weather situations. This parameterisation likely underestimates the gust factor in case of very intense turbulence, which can sometimes occur

#### 4. ADDITION OF A WIND GUST MODULE

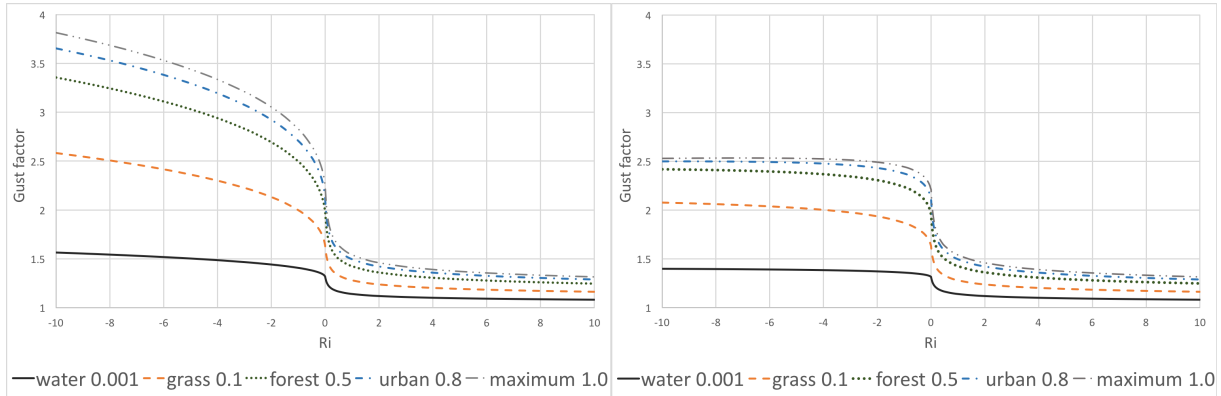


**Figure 7:** Gust factor dependency on the Richardson number for various roughness lengths (m) for the original parameterisation (left panel) and for the modification of the drag calculation by unstable stratification (right panel).

also by stable stratification, e.g., in case of a strong mountain wave flow. The latter case is, however, not applicable for the relatively flat domain of INCA-BE.

Although *observed* wind gusts and gust factors are not incorporated in the procedure yet, the gust scheme does incorporate (observations of) the current atmospheric conditions, via the most recent 10 m wind field and the 3D INCA temperature nowcasts.

## 5 From raw output to forecast applications

### 5.1 INCA-BE web portal for the RMIB forecasters

The INCA core system itself does not include any specific visualisation tailored for its output. A web portal for INCA-BE was built up from the ground. Currently two versions are offered to the end-users: a “classic” version which is rather static, and a contemporary version using more advanced web technologies, allowing for more interaction.

A screenshot of the so-called “classic” interface is shown in Fig. 8. The main navigation control is found in the top left corner, and consists of the “basic”, “precip” (precipitation), “conv” (convection) and “cl” (cloudiness) buttons, corresponding to the subdivision in Table 1. By clicking on (predefined) locations on the map, a meteogram is shown at the bottom of the page for that particular place. The user can also consult the images from the RMIB’s weathercam and snowcam network by hovering the camera icons on the map.

While the “classic” interface was highly appreciated by the forecasters, there was a strong demand for two extra features: (1) the ability to zoom, and (2) the generation of meteograms for any location (not just the predefined ones). To meet these two demands, a new web interface was developed from scratch, using state-of-the-art web technologies, including the open-source mapping library OpenLayers, the charting library Highcharts, a selection of Google Maps APIs, and the Bootstrap CSS framework for styling. A screenshot of this interface is shown in the upper panel of Fig. 9. Clicking on a random place generates a meteogram as shown in the lower panel of Fig. 9.

### 5.2 Integration in the RMIB smartphone app

Since 2015, RMIB offers a free public smartphone app to disseminate its forecasts and warnings on both Android and iOS platforms. The app is location-aware and presents to the user a detailed overview of the expected weather at his/her location, from the nowcast range to the long-term trend. Several forecast sources are incorporated into the back-end of the application, INCA-BE being the most important one for the nowcast range. INCA-BE GRIB files are inserted in a MySQL database in a lat-lon table for fast retrieval of the data, and these data are exposed through a webservice to feed the app. The RMIB smartphone app was installed on more than 1 million devices, with more than 650,000 active users per month (August 2021). Contrary to many similar weather apps, a unique property of the RMIB app is that the RMIB forecasters can adjust and modify the information that is shown to the app users. For example: forecasters can erase false radar echoes in the precipitation nowcast, or they can even adjust forecasted temperatures if conditions are developing differently than predicted in the NWP models.

### 5.3 Return period forecast (INCA-IDF application)

The INCA-IDF application is an attempt to forecast the *severity* of an ongoing precipitation event, by generating a prediction of the event’s return period, considered over different time scales. An early version of this application was originally presented in Reyniers et al. (2010), while a similar approach to generate warnings for regional extreme rainfall was elaborated at

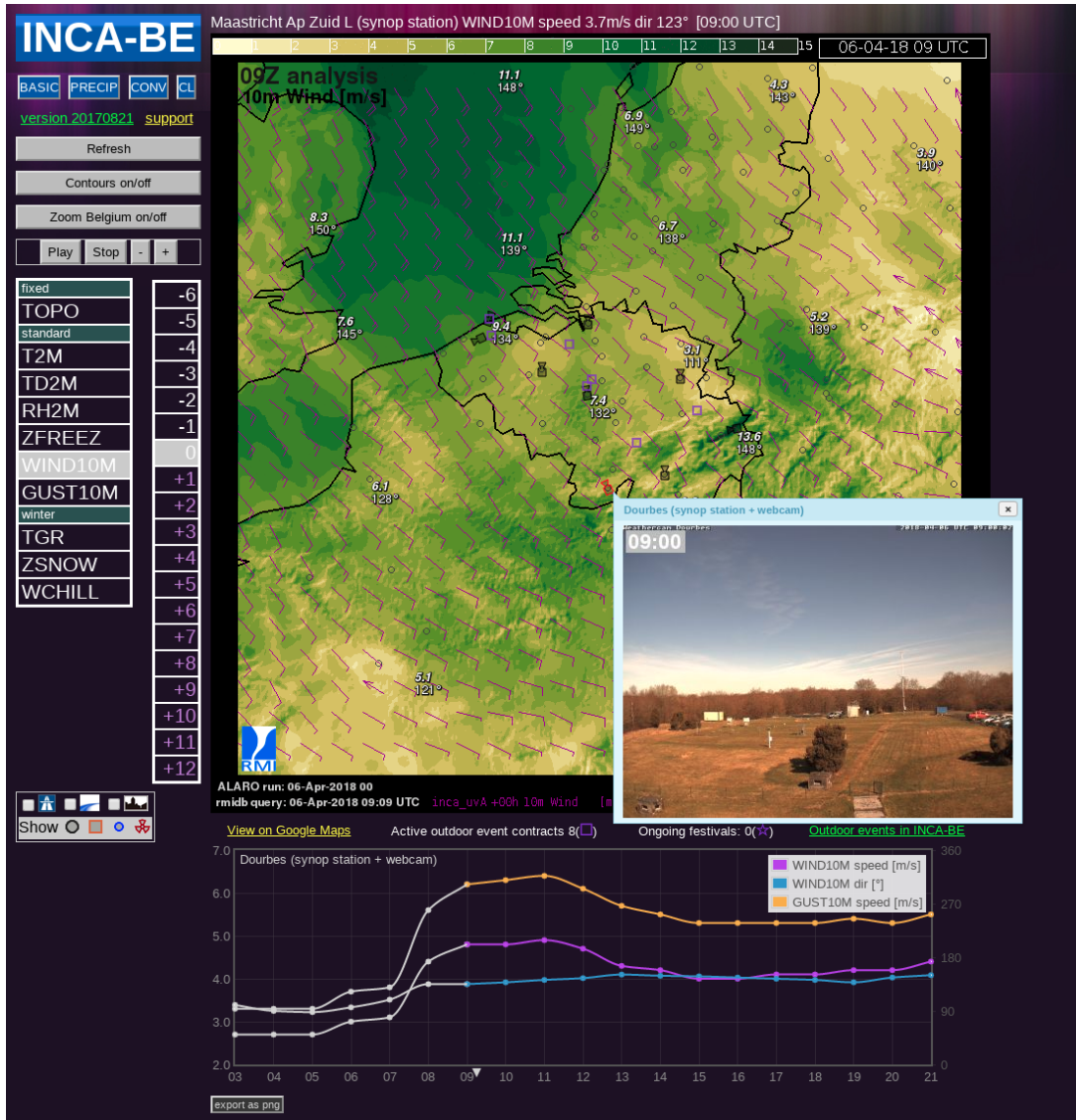


**Figure 8:** Snapshot of the “classic” INCA-BE web interface for the internal users (mainly forecasters) of RMIB, and some selected external users. Meteograms can be generated for (predefined) locations, and images from RMIB’s webcam network can be viewed as well.

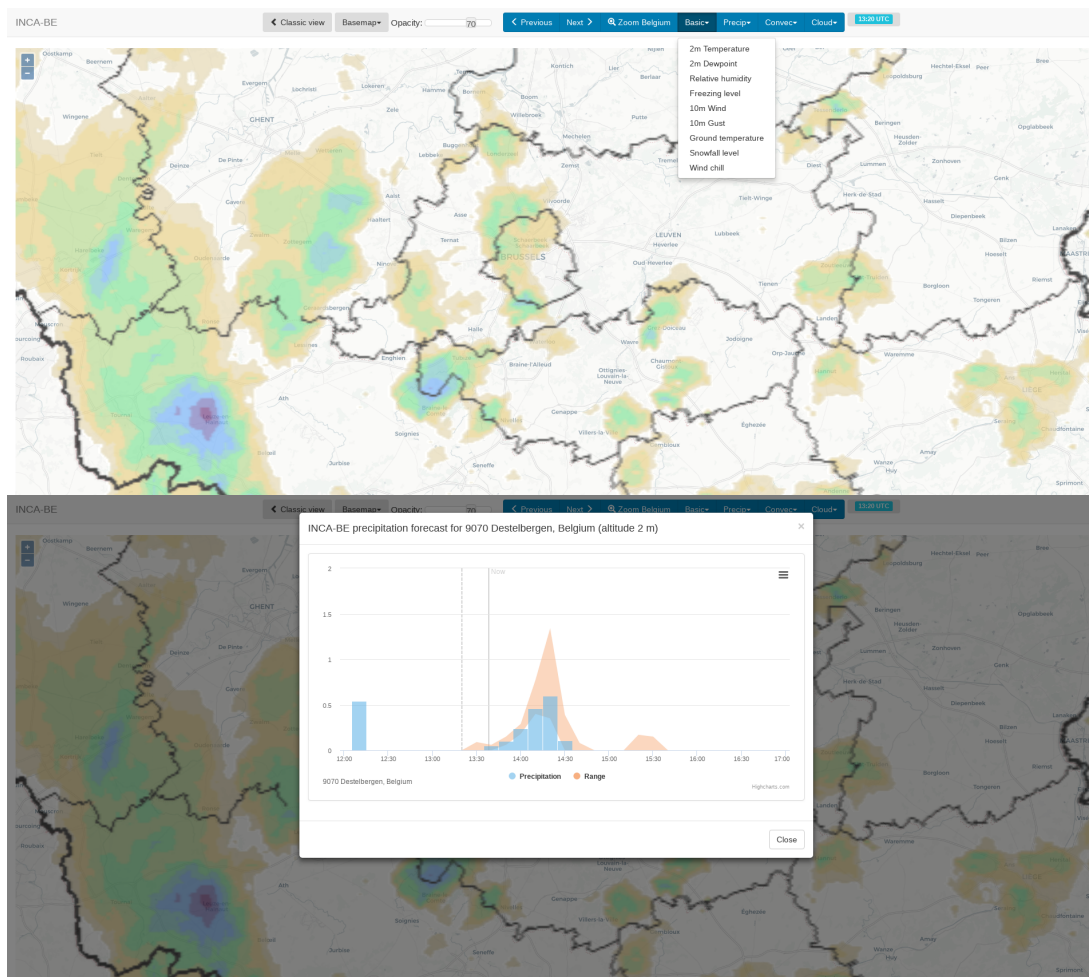


**Figure 9:** Two screenshots of the new, more dynamic INCA-BE web portal which allows more interactivity than the “classic” version shown in Fig 8. The INCA-BE output is displayed on a background map that allows zooming and panning (upper panel). Clicking on a random location activates a pop-up overlay containing an interactive meteogram (lower panel). Background map: © OpenStreetMap contributors.

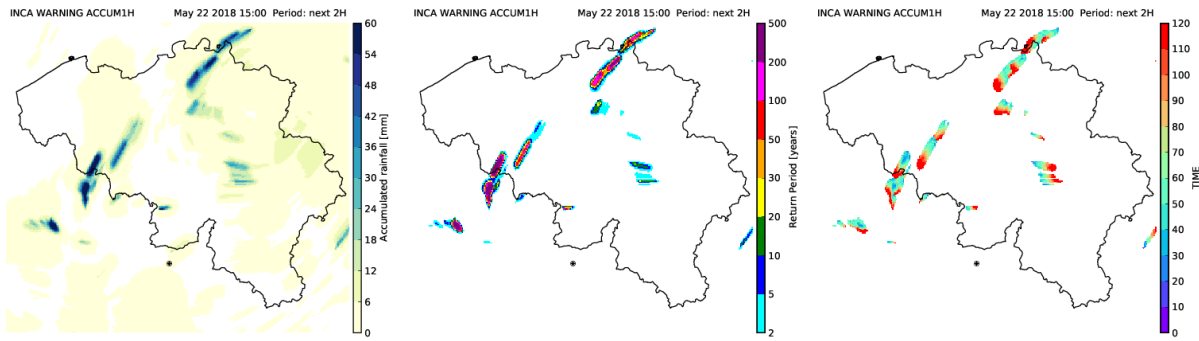


**Figure 10:** The INCA-BE precipitation forecast is further processed in the downstream “INCA-IDF” application, which estimates the severity of an ongoing precipitation event by its return period. To do so, it combines accumulations (with different durations) with Intensity-Duration-Frequency (IDF) information. The INCA-IDF output for the 1 hour accumulation is shown here as an example. The left figure shows the maximum rainfall accumulation for this duration, the middle figure shows the corresponding return period, and the right figure shows the precise timing of this maximum.

MeteoSwiss (Panziera et al., 2016). The INCA-IDF application uses the INCA-BE precipitation forecast between  $t_0$  and  $t_0 + 2h$ , and is updated every ten minutes. Accumulations with four different durations are calculated: 10 min, 30 min, 1h and 3h. Since the nominal time of the output products is the end of the accumulation period, some accumulations contain both past and forecasted precipitation. For example, for the 1h accumulation, the first accumulation corresponds to the period between  $t_0 - 1h$  and  $t_0$ , and the last accumulation between  $t_0 + 1h$  and  $t_0 + 2h$ . Intermediate totals are also calculated and there is for example an hourly accumulation spanning the interval from  $t_0 - 30min$  to  $t_0 + 30min$ . Spatially resolved return period information for Belgium was taken from Van de Vyver (2013).

The evaluation of the severity of an ongoing event is done as follows. The precipitation accumulations for the different nominal times and the different durations are converted into the return periods. For each duration, the maximum accumulation and the corresponding return period give an indication of the severity of an episode in progress. Figure 10 illustrates the different graphical outputs of the INCA-IDF product for the 1h accumulation. The left panel shows the maximum rainfall accumulation for this duration, the middle panel shows the corresponding return period, and the right panel shows the timing of this maximum.

The INCA-IDF application has been proven to be useful in situations where stationary precipitating storm cells are causing extreme local rainfall accumulations with possible flash floods as a result. Propagation of stationary cells is very slow and their speed can be sometimes significantly lower compared to the mean wind speed across the troposphere or compared to the propagation of other storms in the neighbourhood. These situations are, however, hard to recognise on individual radar images or even radar sequences, and are only discovered when forecasters or hydrological operators have advanced products like the INCA-IDF application at their disposal.

#### 5.4 Smartphone notifications for hazardous weather

The January 2020 update of the RMIB smartphone app introduced location-based notifications for hazardous weather. These automatically generated notifications are called “weather

flashes” (and not “warnings”) in order to make a clear distinction with the official warnings manually issued by the RMIB weather office. However, in order to accomplish consistency between both types of information, the weather flashes are generated by mimicking as much as possible the criteria that are used for the official warnings. An important difference is the spatial scale on which the information is disseminated: flashes are issued on the level of a municipality (typically  $\sim 50 \text{ km}^2$ ), while the official warnings are issued on a provincial level (typically  $\sim 3000 \text{ km}^2$ ).

Concerning the temporal scale, two kinds of flashes are defined: the “very short” flashes covering the next 20 minutes, and the “normal” flashes covering a lead time between 20 and 80 minutes ahead. Three different types of hazardous weather are currently covered: (i) thunderstorms with heavy rain, (ii) snowfall, and (iii) freezing rain. In order to produce the flash, several INCA-BE output fields are post-processed by aggregating the output per grid point for both time frames (i.e., for  $[t_0, t_0+20']$  and for  $[t_0+20', t_0+80']$ ). This post-processing is executed for the temperature field, the precipitation field, the lightning field (LF; Section 3.1), and the hail (Section 3.2), snow and freezing rain diagnostics from the precipitation type field.

The next step in this processing is the aggregation, per municipality, of all INCA-BE grid points. In this aggregation, the frequency of occurrence of certain threshold exceedances is calculated. Finally, a flash for a certain municipality is generated if at least 33% of its grid points meet the conditions of the flash. For example, in the case of snowfall, for a certain commune,

- a “normal” flash (lead time 20–80 min) is sent out for “normal” / “intense” / “very intense” snowfall when 33% of the grid points of that commune have a predicted snowfall accumulation that exceeds 1 / 3 / 6 cm, respectively, in the  $[t_0+20', t_0+80']$  time frame;
- a “very short” flash (lead time next 20 min) is sent out for the thresholds 0.4 / 1 / 2 cm as the 10-minute maximum in the  $[t_0, t_0+20']$  time frame.

An additional mechanism is in place to prevent too many flashes during the same event, unless the situation deteriorates considerably. For the moment the different thresholds are chosen mainly based upon the experience of the forecasters and often derived from some specific thresholds used in a legal context. It is the goal to use the return period forecast of Section 5.3 that allows to set consistent thresholds over the different time durations, which leads to a more objective approach in the generation of the flashes.

Most smartphone apps providing weather forecasts offer their users a similar notification service for hazardous weather. An important characteristic that distinguishes the weather flashes included in the RMIB app from their commercial counterparts, is the human supervision of the flash generation. As explained in Section 2.3.3, the filtering of radar images is a very delicate process, and very weak spurious radar echoes, remaining after filtering, can be misinterpreted as snowfall by the system and could provoke false flashes. Also the exact boundary zone where rain transforms into snow (typically in the higher parts of Belgium) can occasionally be ill-defined by a few kilometers due to small uncertainties in the temperature field or due to the specific details of the snow-forming processes. The latter situation can be recognised when the incoming user reports (discussed in Section 3.2) for that particular zone deviate from the INCA-BE predictions as it develops.

For these kind of situations, the forecasters would like to keep control over the flashes, and therefore they have the possibility to evaluate – and ultimately modify – the flashes *before* they are sent out to the app users. For this purpose, they have two clean and simple interfaces at

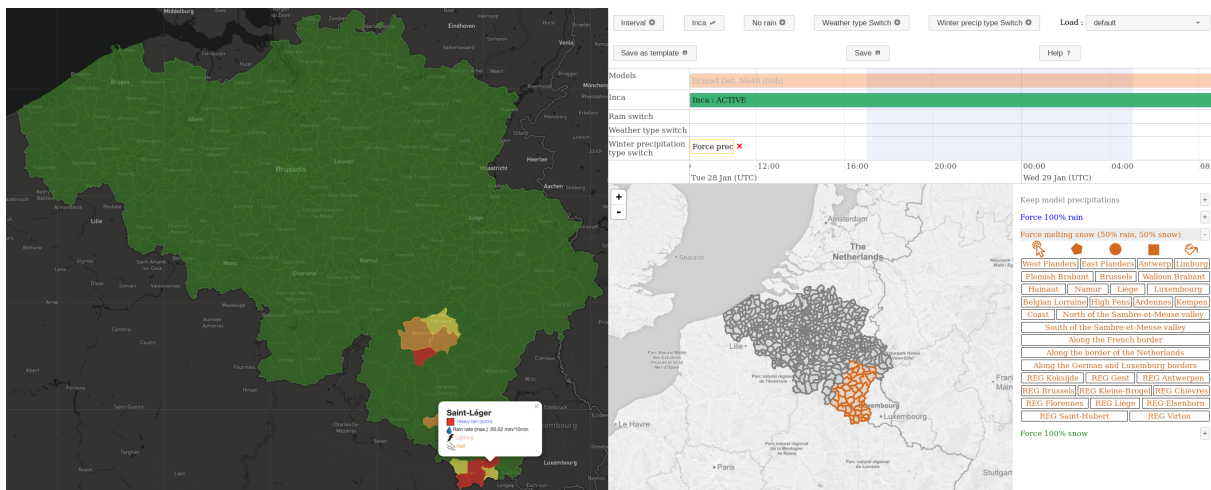


**Figure 11:** Left panel: the forecasters’ view on the pending weather flashes; right panel: the graphical interface that allows the forecasters to manipulate the precipitation type in the generation of the flashes. Background map: © OpenStreetMap contributors.

their disposal: a colour-coded overview map of the active flashes (left panel of Fig 11), and an interactive dashboard (right panel of Fig 11) to adapt the pending flashes. On this dashboard, the forecaster can fine-tune, per municipality, the precipitation type that is prefilled with INCA-BE output.

### 5.5 An interactive, visual monitoring of all model output at RMIB

The archived output of INCA-BE (in GRIB format) has also been incorporated in a visual monitoring tool developed internally at RMIB where it can be compared to output from NWP models and radar data (Fig. 12). The web interface has been coded in R (R Development Core Team, 2011) using the “shiny” package (Chang et al., 2018) for easy development. The interface allows interactive selection of date and time, parameter and various data sources. When comparing NWP forecasts to INCA-BE, one has the option to compare to INCA-BE nowcasts (up to 12h lead time) or to analyses. The main focus of this tool is not on real-time operations but on easy and comprehensive analysis of past cases. In the future, other data sources, e.g., observations and experimental models, can be added to the data selection.

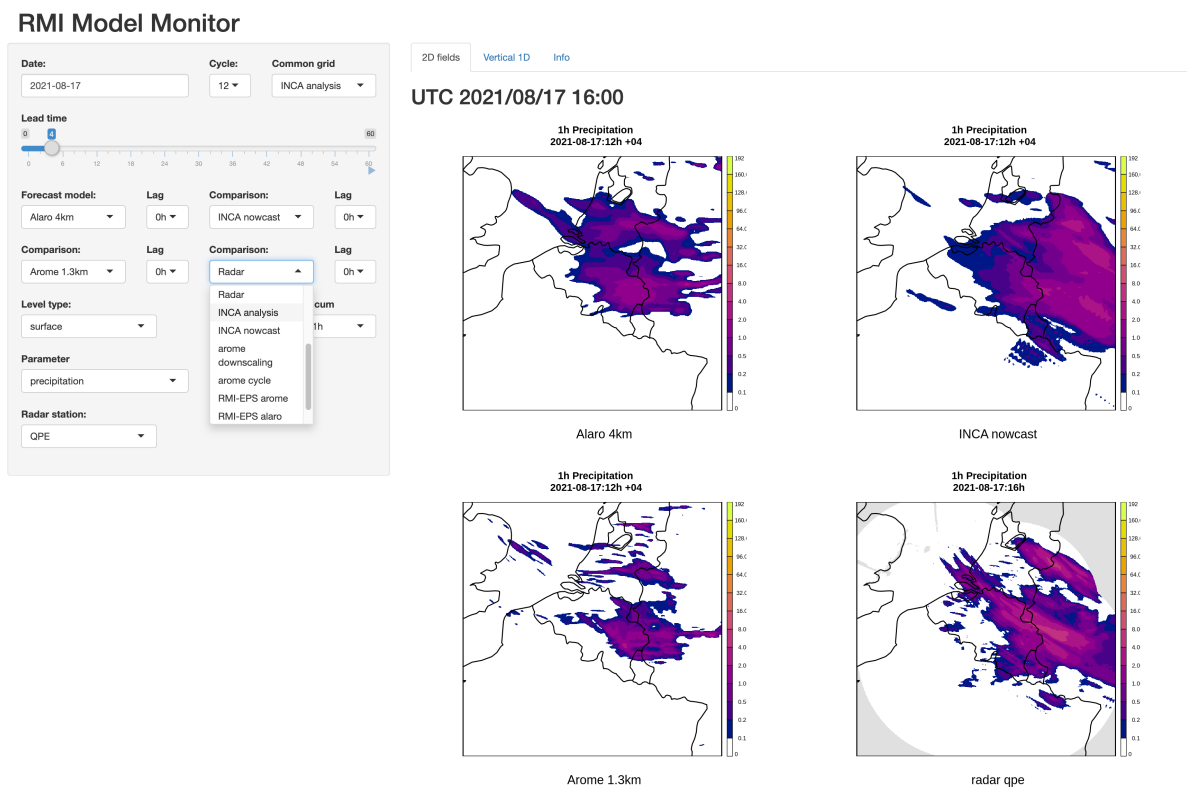


**Figure 12:** A screenshot of the RMIB interactive web monitoring tool showing 1 h accumulated precipitation output of the NWP model ALARO and INCA-BE. For easy comparison, the NWP output has been interpolated on the fly to the INCA-BE grid. Note in the drop-down menu the other sources with which the NWP output can be compared with.

## 6 Overall evaluation

The introduction of INCA-BE into RMIB's operations has been a success story ever since the start of its implementation, now almost ten years ago. The following points have certainly contributed to the success of INCA-BE:

- the availability of the INCA core system provided by ZAMG allowed a rapid deployment of a base system that also served as a benchmark against which subsequent developments were evaluated;
- the development of INCA-BE has largely been driven by a user requirement approach;
- the output of INCA-BE is presented on an intuitive and attractive web portal, which led to a rapid adoption of the system (by, e.g., forecasters), and increased the internal visibility at the level of the institution;
- interaction with the end-users has always been a major point of attention during the whole implementation and development plan: several trainings were organised for the forecasters, but also meetings with external users were organised (e.g., users in hydrology, defence and aviation control).

However, some intrinsic weaknesses were also encountered:

- the absence of a common code repository for developments on top of the INCA core system resulted in diverging national “forks” of the code;
- the INCA core system is proven to be a robust piece of software, but some parts lack critical documentation;
- the deterministic nature of INCA-BE does not allow a rigorous quantification of the uncertainty of the forecast.

In view of the last point, a probabilistic version of INCA, developed in the framework of the PROFORCE project (Wastl et al., 2018), has been tested at ZAMG and OMSZ. At RMIB, the probabilistic precipitation nowcasting system STEPS-BE was implemented (Foresti et al., 2016), in parallel with INCA-BE a few years ago (see also Section 3.4, for a brief discussion). This STEPS version, solely based on radar observations and covering a lead time up to two hours, was made available for our forecasters and some selected external end-users.

A second STEPS version, in which the nowcast ensembles from the radar are blended with the decomposed NWP output from ALARO, is available in test mode. This system, called STEPS-ALARO (De Cruz et al., 2018, 2020), is an important ingredient of RMIB's internal project “IMA”, which aims at the realisation of a seamless, fully probabilistic forecasting system for the 0-12h time range. Currently STEPS-ALARO is built upon the legacy STEPS code (Bowler et al., 2006, and references therein), but we envisage a gradual migration towards the PySTEPS framework (Pulkkinen et al., 2019a,b) in the next years. The new seamless system will also contribute to the mutual coherence of the downstream applications of which a few were presented in Section 5.

## 7 Conclusions and outlook

This technical publication documents the recent developments of the operational nowcasting system INCA-BE to include lightning, hail and wind gusts (Section 3.1, 3.2 and 4, respectively), allowing a considerable improvement of the manual and automatic generation of warnings for meteorological hazards in Belgium (Section 5). The main contribution to the progress in nowcasting is the realisation of an integrated approach of observational, nowcasting and forecasting techniques into one consolidated, robust and widely used nowcasting system, as a bridge between research and operations.

Concerning the future developments of the INCA-BE nowcasting system, the parallel version of INCA-BE in which ALARO is replaced by AROME as base NWP model, was already briefly mentioned in Section 2.3.1. Feature requests from the users, mainly from forecasters but also from hydrologists and road managers, span a wide range of desiderata, ranging from very small adjustments to major system enhancements. Examples of small changes include: add or remove stations from the station list, modifications in the runtime schedule, or fine-tune parameters in the physics of the algorithms. Examples of the more structural change requests are:

- increase the temporal resolution of the hourly fields (Table 1) to 10 min;
- increase the temporal resolution of the precipitation fields from 10 min to 5 min;
- increase the spatial resolution of the INCA-BE grid from 1 km to 500 m;
- add more options in the choice of the utilized base model (currently limited to ALARO and AROME), including the HRES model of ECMWF;
- add the output and extrapolation of some radar-based severe storm signature detection algorithms, similar to the addition of the lightning and hail fields;
- add the analysis and nowcast of wind gusts related to convective storms.

Obviously, apart from these user-driven requests improving the overall system capabilities, technical efforts on the level of the system architecture itself are also necessary, e.g., upgrading the underlying virtual infrastructure on which the software suite is running, migrating from GRIB-1 to GRIB-2 as output format, preparing the software suite for a 64-bit architecture, etc. . . These technical operations, often unnoticed by the end-users if done properly, do require great efforts, and are in many meteorological services an additional responsibility of the nowcasting scientist(s).

While verification efforts have been carried out for both the INCA core system (Haiden et al., 2011) as for its national derivatives, a more systematic quantification of the system performance could be further elaborated. In particular, the verification of the precipitation *type* field is challenging. The collection of citizens' reports through the RMIB smartphone app since August 2019 is a crucial new source of information to advance in this domain. It is the ambition of RMIB to realise considerable progress in this particular field, by combining this novel data source with classical sensing techniques used in meteorology for this purpose, like radar and satellite. The use of crowdsourced data implies the introduction of new challenges concerning data quality and privacy, but at the same time it initiates an exciting new era for nowcasting research and applications.

## Acknowledgments

The members of the scientific committee, *Dieter Poelman*, *Nicolas Clerbaux* and *David Dehenauw*, are warmly thanked for carefully reading the document, and the smooth review process. The successful implementation and continuous improvement of INCA-BE was not possible without the great support of many people and organisations: in the first place my co-authors, *André Simon*, *Laurent Delobbe*, *Alex Deckmyn*, and *Edouard Goudenhoofdt*, but also colleagues *Dieter Poelman*, *Lesley De Cruz*, *Sylvain Watelet*, *David Dehenauw* and *Nicolas Clerbaux* and former colleagues *Maryna Lukach* and *Loris Foresti*; our technical team maintaining the radar and lightning detection systems; *Joffrey Schmitz*, *Stéphane Dekeyzer*, *Alain Tuezney*, *Tom Willems* and the other colleagues of the ICT departement; the forecasters of RMIB, MeteoWing, MeteoLux and the Oceanografisch Meteorologisch Station for feedback in every stage of the implementation; VMM (radar Helchteren), Météo-France (radar Avesnois), DWD (radar Neuheilenbach) and all providers of station data; ZAMG for making available the INCA core system; and finally all international colleagues in the INCA-CE consortium for the great meetings and fruitful collaborations during the INCA-CE project. The maps used as background in Figs. 9 and 11 are available under the Open Database License (<https://www.openstreetmap.org/copyright>).

**Data availability** The INCA-BE output data presented in this study are available on request from the first author free of charge for research purposes. The data are not publicly available due to institutional restrictions.

## List of acronyms

ALADIN	Aire Limitée Adaptation Dynamique Développement International [NWP]
ALARO	ALadinARome [NWP]
AROME	Application of Research to Operations at Mesoscale [NWP]
ARPEGE	Action de Recherche Petite Echelle Grande Echelle [NWP]
AWS	Automatic Weather Station
BELLS	Belgian Lightning Location System
CG	cloud-to-ground
CSI	Critical Success Index
CT	Cloud Type
DWD	Deutscher Wetterdienst
FAR	False Alarm Ratio
GRIB	GRIdded Binary
IC	intra- and intercloud
IDF	Intensity-Duration-Frequency
IMA	RMIB's seamless prediction program for the 0-12 h forecast range
INCA	Integrated Nowcasting through Comprehensive Analysis
INCA-BE	INCA Belgium
INCA-CE	INCA Central Europe
KNMI	Koninklijk Nederlands Meteorologisch Instituut
MCS	Mesoscale Convective System
METRO	Model of the Environment and Temperature of Roads
MSG	Meteosat Second Generation
NWC SAF	Nowcasting Satellite Application Facility
NWP	Numerical Weather Prediction
OMSZ	Országos Meteorológiai Szolgálat
POD	Probability Of Detection
POH	Probability Of Hail
POSH	Probability Of Severe Hail
PROFORCE	Bridging of PRObabilistic FORecasts and Civil protEction
RADQPE	Radar based Quantitative Precipitation Estimation
RMIB	Royal Meteorological Institute of Belgium
RSS	Rapid Scanning Service
RWS	Road Weather Station
SAFIR	Surveillance et Alerte Foudre par Interférométrie Radioélectrique
STEPS-BE	Short-Term Ensemble Prediction System Belgium
VMM	Vlaamse Milieumaatschappij
WMO	World Meteorological Organization
ZAMG	Zentralanstalt für Meteorologie und Geodynamik

## References

- Barras, H., A. Hering, A. Martynov, P.-A. Noti, U. Germann, and O. Martius, 2019: Experiences with >50,000 Crowdsourced Hail Reports in Switzerland. *Bulletin of the American Meteorological Society*, **100** (8), 1429–1440, doi:10.1175/BAMS-D-18-0090.1.
- Bowler, N. E., C. E. Pierce, and A. W. Seed, 2006: Steps: A probabilistic precipitation forecasting scheme which merges an extrapolation nowcast with downscaled nwp. *Quarterly Journal of the Royal Meteorological Society*, **132** (620), 2127–2155, doi:https://doi.org/10.1256/qj.04.100, URL <https://rmets.onlinelibrary.wiley.com/doi/abs/10.1256/qj.04.100>, <https://rmets.onlinelibrary.wiley.com/doi/pdf/10.1256/qj.04.100>.
- Brouwer, T., D. Eilander, A. van Loenen, M. J. Booij, K. M. Wijnberg, J. S. Verkade, and J. Wage-maker, 2017: Probabilistic flood extent estimates from social media flood observations. *Natural Hazards and Earth System Sciences*, **17** (5), 735–747, doi:10.5194/nhess-17-735-2017.
- Chang, W., J. Cheng, J. Allaire, Y. Xie, and J. McPherson, 2018: shiny: Web Application Framework for R. R package version 1.1.0. The R Project, <https://CRAN.R-project.org/package=shiny>.
- Crevier, L.-P. and Y. Delage, 2001: METRo: A new model for road-condition forecasting in canada. *Journal of Applied Meteorology*, **40** (11), 2026–2037, doi:10.1175/1520-0450(2001)040<2026:manmfr>2.0.co;2.
- Debontridder, L., 2008: De frequentie en de diameter van hagelstenen bij onweertijd in belgi tussen 1960 en 2005. Wetenschappelijke en technische publicatie, Nr. 53, Royal Meteorological Institute of Belgium.
- De Cruz, L., A. Deckmyn, D. Degrauwe, I. Dehmous, L. Delobbe, M. Reyniers, P. Termonia<sup>1</sup>, and S. Vannitsem, 2020: Blending of the stochastic precipitation nowcasting system steps-be with an alaro-arome mini-eps at a high spatiotemporal resolution. *11th European Conference on Radar in Meteorology and Hydrology, held in Locarno, Switzerland, postponed to 2022*.
- De Cruz, L., M. Reyniers, L. Delobbe, and L. Foresti, 2018: STEPS-ALARO: Blending high-frequency NWP precipitation forecasts in a stochastic nowcasting system. *15th Annual Meeting of the Asia Oceania Geosciences Society, held in Honolulu, Hawaii*.
- Delobbe, L., I. Holleman, D. Dehenauw, and J. Neméghaire, 2005: Verification of radar-based hail detection products. *Proceedings of the W.W.R.P. Symposium on Nowcasting and Very Short Range Forecasting (WSN05), held in Toulouse, France*.
- Derrien, M., 2014: Product User Manual for “Cloud Products” (CMA-PGE01 v3.2, CTPGE02 v2.2 & CTTH-PGE03 v2.2). Tech. rep., Météo-France, NWC SAF. URL <http://www.nwcsaf.org/>.
- Elmore, K. L., Z. L. Flamig, V. Lakshmanan, B. T. Kaney, V. Farmer, H. D. Reeves, and L. P. Rothfus, 2014: mPING: Crowd-sourcing weather reports for research. *Bulletin of the American Meteorological Society*, **95** (9), 1335–1342, doi:10.1175/bams-d-13-00014.1.
- Fohringer, J., D. Dransch, H. Kreibich, and K. Schröter, 2015: Social media as an information source for rapid flood inundation mapping. *Natural Hazards and Earth System Sciences*, **15** (12), 2725–2738, doi:10.5194/nhess-15-2725-2015.

- Foresti, L., M. Reyniers, A. Seed, and L. Delobbe, 2016: Development and verification of a real-time stochastic precipitation nowcasting system for urban hydrology in Belgium. *Hydrology and Earth System Sciences*, **20** (1), 505–527, doi:10.5194/hess-20-505-2016.
- García-Pereda, J., J. M. Fernández-Serdán, O. Alonso, A. Sanz, R. Guerra, C. Ariza, I. Santos, and L. Fernández, 2019: Nwcsaf high resolution winds (nwc/geo-hrw) stand-alone software for calculation of atmospheric motion vectors and trajectories. *Remote Sensing*, **11** (17), doi:10.3390/rs11172032, URL <https://www.mdpi.com/2072-4292/11/17/2032>.
- Goudenhoofd, E. and L. Delobbe, 2016: Generation and verification of rainfall estimates from 10-yr volumetric weather radar measurements. *Journal of Hydrometeorology*, **17** (4), 1223–1242, doi:10.1175/JHM-D-15-0166.1.
- Haiden, T., A. Kann, G. Pistotnik, K. Stadlbacher, and C. Wittmann, 2010: Integrated nowcasting through comprehensive analysis (inca) - system description. techreport, ZAMG. URL [http://www.zamg.ac.at/fix/INCA\\_system.doc](http://www.zamg.ac.at/fix/INCA_system.doc).
- Haiden, T., A. Kann, C. Wittmann, G. Pistotnik, B. Bica, and C. Gruber, 2011: The integrated nowcasting through comprehensive analysis (INCA) system and its validation over the eastern alpine region. *Weather and Forecasting*, **26** (2), 166–183, doi:10.1175/2010waf2222451.1.
- Holleman, I., 2001: Hail detection using single-polarization radar. Tech. Rep. WR-2001-01, KNMI.
- Jurczyk, A., K. Ordka, J. Szturc, M. Giszterowicz, P. Przeniczny, and G. Tkocz, 2015: Meteorogis: Gis-based system for monitoring of severe meteorological phenomena. *Meteorology Hydrology and Water Management*, **3** (2), 49–61, doi:10.26491/mhwm/60751.
- Karsisto, V., S. Tijn, and P. Nurmi, 2017: Comparing the Performance of Two Road Weather Models in the Netherlands. *Weather and Forecasting*, **32** (3), 991–1006, doi:10.1175/WAF-D-16-0158.1.
- Kyznarov, H., P. Novk, L. Bezkov, P. Janl, and M. Salek, 2013: Precipitation output of inca system: evaluation and use. *European Geosciences Union General Assembly 2013, held in Vienna, Austria, 07–12 April 2013*, URL [https://presentations.copernicus.org/EGU2013/EGU2013-9089\\_presentation.pdf](https://presentations.copernicus.org/EGU2013/EGU2013-9089_presentation.pdf).
- Louis, J.-F., M. Tiedtke, and J.-F. Geleyn, 1982: A short history of the PBL-parameterization at ECMWF. *Workshop on Planetary Boundary Layer parameterization, 25-27 November 1981*, ECMWF, Shinfield Park, Reading, ECMWF, 59–79.
- Lukach, M., L. Foresti, O. Giot, and L. Delobbe, 2017: Estimating the occurrence and severity of hail based on 10 years of observations from weather radar in Belgium. *Meteorological Applications*, **24** (2), 250–259, doi:10.1002/met.1623.
- Panziera, L., M. Gabella, S. Zanini, A. Hering, U. Germann, and A. Berne, 2016: A radar-based regional extreme rainfall analysis to derive the thresholds for a novel automatic alert system in Switzerland. *Hydrology and Earth System Sciences*, **20** (6), 2317–2332, doi:10.5194/hess-20-2317-2016.

- Poelman, D. R., W. Schulz, G. Diendorfer, and M. Bernardi, 2016: The european lightning location system euclid – part 2: Observations. *Natural Hazards and Earth System Sciences*, **16 (2)**, 607–616, doi:10.5194/nhess-16-607-2016, URL <https://nhess.copernicus.org/articles/16/607/2016/>.
- Poelman, D. R., W. Schulz, and C. Vergeiner, 2013: Performance characteristics of distinct lightning detection networks covering belgium. *Journal of Atmospheric and Oceanic Technology*, **30 (5)**, 942–951, doi:10.1175/jtech-d-12-00162.1.
- Pulkkinen, S., D. Nerini, A. Pérez Hortal, C. Velasco-Forero, A. Seed, U. Germann, and L. Foresti, 2019a: pysteps – a community-driven open-source library for precipitation nowcasting. *3rd European Nowcasting Conference (ENC), held in Madrid, Spain. Poster presentation*, doi:10.13140/RG.2.2.31368.67840.
- Pulkkinen, S., D. Nerini, A. A. Pérez Hortal, C. Velasco-Forero, A. Seed, U. Germann, and L. Foresti, 2019b: Pysteps: an open-source python library for probabilistic precipitation nowcasting (v1.0). *Geoscientific Model Development*, **12 (10)**, 4185–4219, doi:10.5194/gmd-12-4185-2019, URL <https://gmd.copernicus.org/articles/12/4185/2019/>.
- R Development Core Team, 2011: *R: A Language and Environment for Statistical Computing*. Vienna, Austria, R Foundation for Statistical Computing, URL <http://www.R-project.org>, ISBN 3-900051-07-0.
- Reyniers, M., 2008: Quantitative precipitation forecasts based on radar observations: principles, algorithms and operational systems. Tech. Rep. 052, Royal Meteorological Institute of Belgium.
- Reyniers, M., L. Delobbe, P. Dierickx, M. Thunus, and C. Tricot, 2010: Storm severity nowcasting by real-time return period imaging. *6th European Conference on Radar in Meteorology and Hydrology, held in Sibiu, Romania. Extended abstract*.
- Saltikoff, E., J. Y. N. Cho, P. Tristant, A. Huuskonen, L. Allmon, R. Cook, E. Becker, and P. Joe, 2016: The threat to weather radars by wireless technology. *Bulletin of the American Meteorological Society*, **97 (7)**, 1159 – 1167, doi:10.1175/BAMS-D-15-00048.1.
- Schulz, W., G. Diendorfer, S. Pedeboy, and D. R. Poelman, 2016: The european lightning location system euclid – part 1: Performance analysis and validation. *Natural Hazards and Earth System Sciences*, **16 (2)**, 595–605, doi:10.5194/nhess-16-595-2016, URL <https://nhess.copernicus.org/articles/16/595/2016/>.
- Seed, A. W., 2003: A dynamic and spatial scaling approach to advection forecasting. *Journal of Applied Meteorology (1988-2005)*, **42 (3)**, 381–388, URL <http://www.jstor.org/stable/26185412>.
- Seity, Y., P. Brousseau, S. Malardel, G. Hello, P. Bénard, F. Bouttier, C. Lac, and V. Masson, 2011: The arome-france convective-scale operational model. *Monthly Weather Review*, **139 (3)**, 976–991, doi:10.1175/2010MWR3425.1.
- Sheridan, P., 2011: Review of techniques and research for gust forecasting and parameterisation. Forecasting Research Technical Report 570, Met Office.

- Simon, A., Á. Horváth, R. Rétfalvi Hodossyné, E. Löwinger, and K. Csirmaz, 2012: Tests of INCA-HU gust calculation. Tech. rep., OMSZ.
- Spruce, M. D., R. Arthur, J. Robbins, and H. T. P. Williams, 2021: Social sensing of high-impact rainfall events worldwide: A benchmark comparison against manually curated impact observations. *Natural Hazards and Earth System Sciences Discussions*, **2021**, 1–31, doi:10.5194/nhess-2020-413.
- Stauffer, R., G. J. Mayr, M. Dabernig, and A. Zeileis, 2015: Somewhere over the rainbow: How to make effective use of colors in meteorological visualizations. *Bulletin of the American Meteorological Society*, **96** (2), 203–216, doi:10.1175/bams-d-13-00155.1.
- Stoelzle, M. and L. Stein, 2021: Rainbow color map distorts and misleads research in hydrology – guidance for better visualizations and science communication. *Hydrology and Earth System Sciences*, **25** (8), 4549–4565, doi:10.5194/hess-25-4549-2021, URL <https://hess.copernicus.org/articles/25/4549/2021/>.
- Termonia, P., et al., 2018: The ALADIN system and its canonical model configurations AROME CY41t1 and ALARO CY40t1. *Geoscientific Model Development*, **11**, 257–281, doi:10.5194/gmd-11-257-2018.
- Thyng, K., C. Greene, R. Hetland, H. Zimmerle, and S. DiMarco, 2016: True colors of oceanography: Guidelines for effective and accurate colormap selection. *Oceanography*, **29** (3), 9–13, doi:10.5670/oceanog.2016.66.
- Van de Vyver, H., 2013: Practical return level mapping for extreme precipitation in Belgium. Tech. Rep. 062, Royal Meteorological Institute of Belgium.
- Wang, Y., et al., 2017: Integrating nowcasting with crisis management and risk prevention in a transnational and interdisciplinary framework. *Meteorologische Zeitschrift*, **26** (5), 459–473, doi:10.1127/metz/2017/0843.
- Wastl, C., et al., 2018: A seamless probabilistic forecasting system for decision making in civil protection. *Meteorologische Zeitschrift*, **27** (5), 417–430, doi:10.1127/metz/2018/902.
- Witt, A., M. D. Eilts, G. J. Stumpf, J. T. Johnson, E. D. W. Mitchell, and K. W. Thomas, 1998: An enhanced hail detection algorithm for the WSR-88D. *Weather and Forecasting*, **13** (2), 286–303, doi:10.1175/1520-0434(1998)013<0286:aehdaf>2.0.co;2.
- WMO, 1994: A guide to the code form FM 92-IX Ext. GRIB Edition 1. Tech. Rep. No.17, Geneva, May 1994 (WMO TD-No.611), WMO.
- WMO, 2017: Guidelines for nowcasting techniques. Tech. Rep. No. 1198, WMO.
- Zabini, F., 2016: Mobile weather apps or the illusion of certainty. *Meteorological Applications*, **23** (4), 663–670, doi:10.1002/met.1589.

**The INCA-BE system: ten years of operational nowcasting and  
its applications at the national meteorological service of Belgium**

**Maarten Reyniers, André Simon, Laurent Delobbe, Alex Deckmyn, Edouard Goudenhoofd**

DOI: [10.5281/zenodo.5798952](https://doi.org/10.5281/zenodo.5798952)

Koninklijk Meteorologisch Instituut van België  
Institut Royal Météorologique de Belgique  
Königliches Meteorologisches Institut von Belgien  
Royal Meteorological Institute of Belgium